

Ball Lightning as a profound manifestation of the Dark Matter physics

Ariel Zhitnitsky

Department of Physics and Astronomy, University of British Columbia, Vancouver, V6T 1Z1, BC, Canada

Abstract

Ball lighting (BL) has been observed for centuries. There are large number of books, review articles, and original scientific papers devoted to different aspects of BL phenomenon. Yet, the basic features of this phenomenon have never been explained by known physics. The main problem is the source which could power the dynamics of the BL. We advocate an idea that the dark matter (DM) in form of the axion quark nuggets (AQN) made of standard model quarks and gluons (similar to the old idea of the Witten's strangelets) could internally generate the required power. The AQN model was invented long ago without any relation to the BL physics. It was invented with a single motivation to explain the observed similarity $\Omega_{\text{DM}} \sim \Omega_{\text{visible}}$ between visible and DM components. This relation represents a very generic feature of this framework, not sensitive to any parameters of the construction. However, with the same set of parameters being fixed long ago this model is capable to address the key elements of the BL phenomenology, including the source of the energy powering the BL events. In particular, we argue that the visible size of BL, its typical life time, the frequency of appearance, etc are all consistent with suggested proposal when BL represents a profound manifestation of the DM physics represented by the AQN objects. We also argue that some of the Unidentified Aerial Phenomena (UAP) might be closely related to BL events, and therefore also represent profound manifestations of the DM physics within AQN framework. We also formulate a number of specific possible tests which can refute or unambiguously substantiate this unorthodox proposal on nature of BL and UAP.

Key words: dark matter, axion, quark nugget, antimatter nuggets, ball lighting

1. Introduction

The title of this work seemingly includes two contradicting terms: the first one is “ball lighting”, which is very bright luminous object, though of unknown nature. The second term of the title is “dark matter” (DM) which is, by definition, must decouple from the radiation, as it cannot emit light. Indeed, the BL phenomenon has been known for centuries, see recent book [1] and review papers [2–4] with large number of references therein. See also recent review article [5] with several historical comments on BL observations by scientists and trained professionals. The main goal of this work is to argue that the numerous puzzling observations of the ball lighting (BL) could be explained from unified viewpoint within a specific dark matter model, the so-called axion quark nugget (AQN) dark matter model [6], see also brief review [7] for a short overview of the AQN framework.

We overview the basic ideas of the AQN construction in next section. The main outcome of this construction is that the AQN behaves as a chameleon: it serves as a proper DM object in dilute environment, but becomes very strongly interacting object when it hits the stars or planets. Therefore, the contradiction in the title is only apparent as the DM in form of the AQNs become strongly interacting objects in dense environment and can indeed produce profound and very powerful events such as BL, which is the topic of the present work.

Before we proceed with our explanations of the BL phenomenology within AQN framework we should, first of all, highlight the mysterious properties of the observations [1–4] which are impossible to understand if interpreted in terms of the conventional physics. In fact a complete failure to understand even the very basic features of the BL phenomenology (such as required power, or passing through a solid glass) enforced

the researchers to look for possible answers to subatomic physics, well outside the conventional mechanisms considered in the past. In particular, in ref. [8] it was suggested that the magnetic monopole might be powering the BL, while in ref. [9] this idea was modified by adding an electrical charge into the system by making the dyon (magnetic monopole with non-vanishing electric charge). Our proposal is also deeply rooted into subatomic physics, but in dramatically different way, as we discuss below.

1.1. Brief overview of ball lightning phenomenology

The first term of the title is “ball lightning”. Therefore, we have to explain and list the basic features of BL. We literally follow (quote) the review article [4] which states that a successful model should explain the following observed features:

- (i) ball lightning’s association with thunderstorms or with cloud-to-ground lightning;
- (ii) its reported shape, diameter, and duration, and the fact that its size, luminosity, and appearance generally do not change much throughout its lifetime;
- (iii) its occurrence in both open air and in enclosed spaces such as buildings or aircraft;
- (iv) the fact that ball lightning motion is inconsistent with the convective behaviour of a hot gas;
- (v) the fact that it may decay either silently or explosively;
- (vi) the fact that ball lightning does not often cause damage;
- (vii) the fact that it appears to pass through small holes, through metal screens, and through glass windows;
- (viii) the fact that it is occasionally reported to produce acrid odors and/or to leave burn marks, is occasionally described as producing hissing, buzzing, or fluttering sounds, and is sometimes observed to rotate, roll, or bounce off the ground.

In addition to these well established features of the BL we want to add few very important recent quantitative measurements suggesting that there is a new scale of the problem on the level $240\mu m$ [10]. Studies were performed with optical and scanning microscopes and laser beam probing of the glass that experienced action of 20 cm BL. Furthermore, the spectrum from BL has been observed with two slitless spectrographs at a distance 0.9 km, and it includes the soil components (Si I, Fe I, Ca I) as well as the air components (N I, O I) [11, 12]. Furthermore, it has been recently claimed that BL radiation must be accompanied by UV or even X ray emission[13]. Therefore we add few more items to the list:

- (ix) new scale emerges in the BL problem: $240\mu m$ which is dramatically different from the visible size of the BL [10];
- (x) spectrum from BL includes lines from soil components (Si I, Fe I, Ca I) as well as the air components (N I, O I) [11, 12].
- (xi) spectrum from BL must include UV or/and x ray emission [13].

We also want to list some BL’s characteristics which had been collected for decades and which play very important role in our discussions. We start with energetic characteristics of the BL. The energies of the BL events dramatically vary from case to case and can be estimated as follows [2]:

$$E_{\min} = 10^{-0.8\pm 0.2} \text{ kJ}, \quad E_{\max} = 10^{3.2\pm 0.2} \text{ kJ}, \quad \bar{E} = 10^{1.3\pm 0.2} \text{ kJ}. \quad (1)$$

The energy density ϵ also varies for different observations and has been estimated as [2]:

$$\epsilon_{\min} = 10^{-0.6\pm 0.5} \frac{J}{\text{cm}^3}, \quad \epsilon_{\max} = 10^{3\pm 0.5} \frac{J}{\text{cm}^3}, \quad \bar{\epsilon} = 10^{1.2\pm 0.5} \frac{J}{\text{cm}^3}. \quad (2)$$

Typical diameter of the BL has been estimated as [2]:

$$d = 28 \pm 4 \text{ cm}, \quad (3)$$

while life time τ and velocity v_{BL} have been estimated from variety of observations as [2]:

$$\tau = 9_{-4}^{+6} \text{ s}, \quad v_{\text{BL}} \in (0.1 - 10) \frac{\text{m}}{\text{s}}, \quad \bar{v}_{\text{BL}} = 4 \frac{\text{m}}{\text{s}}. \quad (4)$$

Another important parameter we need for our discussions is the radiated power (extracted from studies of the visible frequency bands) which also strongly varies, and on average can be estimated as [2]:

$$P = 10^{2.0\pm 0.2} \text{ W}. \quad (5)$$

The main obstacle preventing the development of a successful BL phenomenology is failure to explain the source of required energy. Any conventional theory (including any known sources of energy) cannot explain one particular well-established property of ball lightning: its ability to pass through closed glass windows [14]. The authors of ref. [10] arrived to a similar conclusion by analyzing the glass damaged by passing BL using the scanning electron microscope as listed in item (ix) above. The only physical entities which can easily pass through a few mm of solid glass are subatomic particles, which recently motivated the authors of refs [8] and [9] to consider the magnetic monopole as a possible source of BL’s energy powering its dynamics.

1.2. Brief overview of dark matter

The second term of the title is “dark matter”. Therefore, we have to briefly explain the term “dark matter”. From cosmological viewpoint there is a fundamental difference between dark matter and ordinary matter (aside from the trivial difference dark vs. visible). Indeed, DM played a crucial role in the formation of the present structure in the universe. Without dark matter, the universe would have remained too uniform to form the galaxies. Ordinary matter could not produce fluctuations to create any significant structures because it remains tightly coupled to radiation, preventing it from clustering, until recent epochs. The key parameter which enters all the cosmological observations is the corresponding cross section σ (describing coupling of DM with standard model particles) to mass M_{DM} ratio which must be sufficiently small to play the role of the DM as briefly mentioned above, see e.g. recent review [15]:

$$\frac{\sigma}{M_{\text{DM}}} \ll 1 \frac{\text{cm}^2}{\text{g}}. \quad (6)$$

The Weakly Interacting Massive Particles (WIMP) obviously satisfy to the criteria (6) to serve as DM particles due to their very tiny cross section σ for a typical mass $M_{\text{WIMP}} \in (10^2 - 10^3)$ GeV. However, the WIMP paradigm which has been the dominant idea for the last 40 years has failed as dozen of dedicated instruments could not find any traces of WIMPs though the sensitivity of the instruments had dramatically improved by many orders of magnitude during the last decades.

In the present work we consider a fundamentally different type of the DM which is in form of macroscopically large composite objects of nuclear density, similar to the Witten’s quark nuggets [16–18]. The corresponding objects are called the axion quark nuggets (AQN) and behave as *chameleons*: they (almost) not interacting entities in dilute environment, such that the AQNs may serve as proper DM candidates as the corresponding condition (6) is perfectly satisfied for the AQNs during the structure formation when the ratio $\sigma/M_{\text{AQN}} \leq 10^{-10} \text{cm}^2 \text{g}^{-1}$, see (7). However, the same objects interact very strongly with material when they hit the Earth, or other planets and stars.

The main distinct feature of the AQN model (which plays absolutely crucial role for the present work) in comparison with old Witten’s construction is that AQNs can be made of *matter* as well as *antimatter* during the QCD transition as a result of the charge segregation process, see brief overview [7]. This charge segregation mechanism separates quarks from antiquarks during the QCD transition in early Universe as a result of dynamics of the \mathcal{CP} odd axion field, see more detail explanations and references in next Sect.2. This separation of baryon charges lead to formation of the quark nuggets and anti-quark nuggets with a similar rate.

The presence of the antimatter nuggets in the system implies that there will be annihilation events leading to very profound strong effects when antimatter AQNs hit the Earth. Our claim here is that the basic features of the BL phenomenology as listed by items (i)- (xi) along with basic BL’s characteristics expressed by (1)-(5) may naturally emerge as a result of these powerful and energetic annihilation events.

We reiterate the main claim of this work slightly differently: our proposal is that the source of energy which is powering BL events is related to the annihilation events of the antimatter hidden in form of the AQNs with surrounding atoms and molecules¹. The fuel which is powering the BL physics is the antimatter nuggets which had been formed during the QCD transition in early Universe. It has been also shown that

¹In fact, the antimatter as a possible source of the energy powering BL has been discussed long ago [19, 20]. I thank Karl Stephan for pointing out into these two old papers.

the dominant fraction of these antimatter nuggets mostly survive until present epoch, see brief review on formation mechanism and survival pattern in next Sect. 2.1.

This model was invented long ago to resolve fundamental problems in cosmology, not related in any way to BL phenomena (in contrast with numerous proposals which were specifically designed to explain different aspects of the BL phenomenology). Nevertheless, this AQN framework may also shed a light to another long standing problem which is the nature of the BL. We stress that all parameters for this model were fixed long ago in our previous applications to explain some mysterious and puzzling observations at galactic and solar scales, to be reviewed in Conclusion in Sect. 6.3. We keep all these parameters of the AQN model identically the same and we do not attempt to modify them to better fit the observations related to BL phenomenology.

The presentation of this work is organized as follows. Next Sect. 2 represents a brief overview of the AQN construction. In our main Sect. 3 we argue that the various of observations as formulated above and collected for decades can be naturally explained within AQN framework. In Sect. 4 we estimate the BL event rate and find it is consistent with observations. In Sect. 5 we argue that some of the Unidentified Aerial Phenomena (UAP) might be closely related to BL events, and therefore also represent profound manifestations of the DM physics. In our concluding Sect. 6 we suggest a number of specific tests which can substantiate or refute our proposal on close relation between BL, UAP and dark matter physics within AQN framework.

2. The AQN dark matter model

We overview the fundamental ideas of the AQN model in subsection 2.1, while in subsections 2.2 and 2.3 we list some specific features of the AQNs relevant to the present work.

2.1. The basics

The original motivation for the AQN model can be explained as follows. It is commonly assumed that the Universe began in a symmetric state with zero global baryonic charge and later (through some baryon-number-violating process, non-equilibrium dynamics, and \mathcal{CP} -violation effects, realizing the three famous Sakharov criteria) evolved into a state with a net positive baryon number.

As an alternative to this scenario, we advocate a model in which “baryogenesis” is actually a charge-separation (rather than charge-generation) process in which the global baryon number of the universe remains zero at all times. This represents the key element of the AQN construction.

In other words, the unobserved antibaryons in visible sector in this model comprise dark matter being in the form of dense nuggets of antiquarks and gluons in the colour superconducting (CS) phase. The result of this “charge-separation process” are two populations of AQN carrying positive and negative baryon number. The global \mathcal{CP} violating processes associated with the so-called initial misalignment angle θ_0 which was present during the early formation stage, the number of nuggets and antinuggets will be different. This difference is always an order-of-one effect irrespective of the parameters of the theory, the axion mass m_a or the initial misalignment angle θ_0 .

The presence of the antimatter nuggets in the AQN framework is an inevitable and the direct consequence of the \mathcal{CP} violating axion field which is present in the system during the QCD time. As a result of this feature the DM density, Ω_{DM} , and the visible density, Ω_{visible} , will automatically assume the same order of magnitude densities $\Omega_{\text{DM}} \sim \Omega_{\text{visible}}$ irrespective to the parameters of the model, such as the axion mass m_a . This feature represents a generic property of the construction [6, 7].

This type of DM is “cosmologically dark” as a result of smallness of the parameter (6) relevant for cosmology. This numerically small ratio scales down many observable consequences of an otherwise strongly-interacting DM candidate in form of the AQN nuggets. Indeed, for a typical AQN parameters the relevant ratio assumes the following numerical value:

$$\frac{\sigma}{M_N} \sim \frac{\pi R^2}{M_N} \sim 10^{-10} \frac{\text{cm}^2}{\text{g}}, \quad (7)$$

Property	Typical value or feature
AQN's mass $[M_N]$	$M_N \approx 16 g (B/10^{25})$ [7]
baryon charge constraints $[B]$	$B \geq 3 \cdot 10^{24}$ [7]
annihilation cross section $[\sigma]$	$\sigma \approx \kappa \pi R^2 \simeq 1.5 \cdot 10^{-9} \text{cm}^2 \cdot \kappa (R/2.2 \cdot 10^{-5} \text{cm})^2$
density of AQNs $[n_{\text{AQN}}]$	$n_{\text{AQN}} \sim 0.3 \cdot 10^{-25} \text{cm}^{-3} (10^{25}/B)$ [7]
survival pattern during BBN	$\Delta B/B \ll 1$ [26–29]
survival pattern during CMB	$\Delta B/B \ll 1$ [26, 28, 30]
survival pattern during post-recombination	$\Delta B/B \ll 1$ [25]

Table 1: Basic properties of the AQNs adopted from [31]. The parameter κ in Table is introduced to account for possible deviation from geometric value πR^2 as a result of ionization of the AQNs due to interaction with environment. The ratio $\Delta B/B \ll 1$ in the Table implies that only a small portion ΔB of the total (anti)baryon charge B hidden in form of the AQNs get annihilated during big-bang nucleosynthesis (BBN), Cosmic Microwave Background (CMB), or post-recombination epochs (including the galaxy and star formation), while the dominant portion of the baryon charge survives until the present time.

where for numerical estimate we use parameters from Table 1 to be discussed below. It obviously satisfies the cosmological constraint (6).

Another important characteristic is the AQN flux which we need in what follows to estimate the BL occurrency rate. It can be estimated as follows [21]:

$$\frac{d\Phi}{dA} = \frac{\Phi}{4\pi R_{\oplus}^2} = 4 \cdot 10^{-2} \left(\frac{10^{25}}{\langle B \rangle} \right) \frac{\text{events}}{\text{yr} \cdot \text{km}^2}, \quad (8)$$

where $R_{\oplus} = 6371 \text{ km}$ is the radius of the Earth, while $\langle B \rangle \approx 10^{25}$ is a typical baryon charge of the AQNs from Table 1 to be discussed below, and Φ is the total hit rate of AQNs on Earth [21]:

$$\Phi \approx \frac{2 \cdot 10^7}{\text{yr}} \left(\frac{\rho_{\text{DM}}}{0.3 \text{ GeV cm}^{-3}} \right) \left(\frac{v_{\text{AQN}}}{220 \text{ km s}^{-1}} \right) \left(\frac{10^{25}}{\langle B \rangle} \right), \quad (9)$$

where ρ_{DM} is the local density of DM within Standard Halo Model (SHM).

We refer to the original papers [22–25] devoted to the specific questions related to the nugget's formation, generation of the baryon asymmetry, and survival pattern of the nuggets during the evolution in early Universe with its unfriendly environment. In particular, the absolute stability of the AQNs in vacuum is a result of the construction when the energy per baryon charge in the quark-matter nuggets is smaller than in the baryons (from hadronic phase) making up the visible portion of the Universe.

This construction is consistent with all presently available cosmological, astrophysical and terrestrial constraints as long as the average baryon charge of the nuggets is sufficiently large as we review below. Precisely the presence of the antimatter nuggets make the AQNs to be very strongly interacting objects as a result of annihilation of the AQNs with surrounding material when AQNs hit stars or planets.

In the AQN scenario the DM density, Ω_{DM} representing the matter and anti-matter nuggets, and the visible density, Ω_{visible} , will automatically assume the same order of magnitude densities $\Omega_{\text{DM}} \sim \Omega_{\text{visible}}$ as they both proportional to one and the same fundamental dimensional parameter of the theory, the Λ_{QCD} . Therefore, the AQN model, by construction, actually resolves two fundamental problems in cosmology (explains the baryon asymmetry of the Universe, and the presence of DM with proper density $\Omega_{\text{DM}} \sim \Omega_{\text{visible}}$) without necessity to fit any parameters of the model.

The strongest direct detection limit² is set by the IceCube Observatory's, see Appendix A in [21]:

$$\langle B \rangle > 3 \cdot 10^{24} \quad [\text{direct (non)detection constraint}]. \quad (10)$$

²Non-detection of etching tracks in ancient mica gives another indirect constraint on the flux of DM nuggets with mass $M > 55g$ [32]. This constraint is based on assumption that all nuggets have the same mass, which is not the case for the AQN model.

The basic idea of the constraint (10) is that IceCube with its surface area $\sim \text{km}^2$ has not detected any events during its 10 years of observations. In the estimate (10) it was assumed that the efficiency of detection of a macroscopically large nugget is 100% which excludes AQNs with small baryon charges $\langle B \rangle < 3 \cdot 10^{24}$ with $\sim 3.5\sigma$ confidence level.

The authors of Ref. [28] considered a generic constraint for the nuggets made of antimatter (ignoring all essential specifics of the AQN model such as quark matter colour superconducting (CS) phase of the nugget's core, see [33] for introduction of the CS phases.). Our constraints (10) are consistent with their findings including the Cosmic Microwave Background (CMB) and Big Bang Nucleosynthesis (BBN), and others, except the constraints derived from the so-called ‘‘Human Detectors’’. As explained in [34] the corresponding estimates of Ref. [28] are oversimplified and do not have the same status as those derived from CMB or BBN constraints.

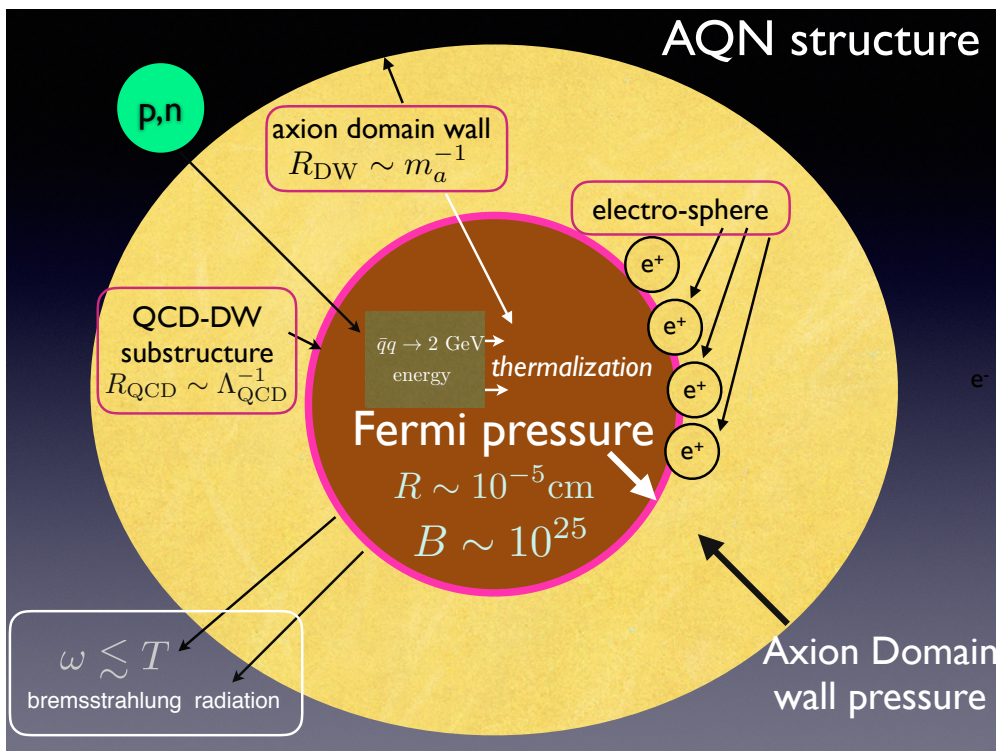


Figure 1: AQN-structure (not in scale), adopted from [35]. The dominant portion of the energy $\sim 2 \text{ GeV}$ produced as a result of a single annihilation process inside the anti-nugget is released in form of the bremsstrahlung radiation with frequencies $\omega \leq T$, see description and notations in the main text.

We draw the AQN-structure on Fig 1, where we use typical parameters from the Table 1. There are several distinct length scales of the problem: $R \sim 10^{-5} \text{ cm}$ represents the size of the nugget filled by dense quark matter with total baryon charge $B \sim 10^{25}$ in CS phase. Much larger scale $R_{\text{DW}} \sim m_a^{-1}$ describes the axion DW surrounding the quark matter. The axion DW has the QCD substructure surrounding the quark matter and which has typical width of order $R_{\text{QCD}} \sim 10^{-13} \text{ cm}$. Finally, there is always electro-sphere which represents a very generic feature of quark nuggets, including the Witten's original construction. In case of antimatter-nuggets the electro-sphere comprises the positrons. The typical size of the electro-sphere is order of 10^{-8} cm .

We conclude this brief review subsection with Table 1 which summarizes the basic features and parameters of the AQNs. Important point here is that only a small portion $\Delta B \ll B$ of the total (anti)baryon charge B hidden in form of the AQNs get annihilated during long evolution of the Universe, while the dominant portion of the baryon charge survives until the present time.

2.2. When the AQN hits the Earth

The computations of the AQN-visible matter interaction originally have been carried out in [36] in application to the galactic environment with a typical density of surrounding baryons of order $n_{\text{galaxy}} \sim \text{cm}^{-3}$ in the galaxy. We review these computations below with few additional elements which must be implemented in case of propagation of the AQN in denser environment such as Earth's atmosphere with $n_{\text{atm}} \sim 10^{21} \text{cm}^{-3}$.

When the AQN enters the region of the baryon density n the annihilation processes start and the internal temperature increases. A typical internal temperature T of the AQN can be estimated from the condition that the radiative output must balance the flux of energy onto the nugget [36]:

$$F_{\text{tot}}(T)(4\pi R^2) \approx \kappa \cdot (\pi R^2) \cdot (2 \text{ GeV}) \cdot n \cdot v_{\text{AQN}}, \quad (11)$$

where n represents the baryon number density of the surrounding material, and $F_{\text{tot}}(T)$ is total surface emissivity, see below. The left hand side accounts for the total energy radiation from the AQN's surface per unit time while the right hand side accounts for the rate of annihilation events when each successful annihilation event of a single baryon charge produces $\sim 2m_p c^2 \approx 2 \text{ GeV}$ energy. The factor κ in (11) accounts for large theoretical uncertainties related to the annihilation processes of the (antimatter) AQN colliding with surrounding material.

The total surface emissivity due to the bremsstrahlung radiation from electrosphere at temperature T has been computed in [36] and it is given by

$$F_{\text{tot}} \approx \frac{16}{3} \frac{T^4 \alpha^{5/2}}{\pi} \sqrt[4]{\frac{T}{m}}, \quad (12)$$

where $\alpha \approx 1/137$ is the fine structure constant, $m = 511 \text{ keV}$ is the mass of electron, and T is the internal temperature of the AQN. One should emphasize that the emission from the electrosphere is not thermal, and the spectrum is dramatically different from blackbody radiation.

As we mentioned above, the thermal properties in (11), (12) were originally applied to the study of the emission from AQNs from the Galactic Centre, where a nugget's internal temperature is very low, $T \sim \text{eV}$. When the nuggets propagate in the Earth's atmosphere, the AQN's internal temperature starts to rise up to $\sim 20 \text{ keV}$ or so. From (11) one can estimate a typical internal nugget's temperature in the Earth atmosphere as follows:

$$T \sim 20 \text{ keV} \cdot \left(\frac{n_{\text{air}}}{10^{21} \text{ cm}^{-3}} \right)^{\frac{4}{17}} \left(\frac{\kappa}{0.1} \right)^{\frac{4}{17}}, \quad (13)$$

where typical density of surrounding baryons is $n_{\text{air}} \simeq 30 \cdot N_m \simeq 10^{21} \text{ cm}^{-3}$, where $N_m \simeq 2.7 \cdot 10^{19} \text{ cm}^{-3}$ is the molecular density in atmosphere when each molecule contains approximately 30 baryons. Thus, in the atmosphere the internal nugget's temperature $T \approx 20 \text{ KeV}$. Similar temperature $T \approx 20 \text{ keV}$ had been previously used in [37] to explain the unusual Cosmic Ray like events observed by Telescope Array Collaboration (so-called "TA bursts"), and in [35] to explain "Exotic Events" recorded by the AUGER collaboration.

Another feature which is relevant for our present studies is the ionization properties of the AQN. Ionization, as usual, occurs in a system as a result of the high internal temperature T . In our case of the AQN characterized by temperature (13) a large number of weakly bound positrons $\sim Q$ from the electrosphere get excited and can easily leave the system. The corresponding parameter Q can be estimated as follows:

$$Q \approx 4\pi R^2 \int_0^\infty n(z, T) dz \sim \frac{4\pi R^2}{\sqrt{2\pi\alpha}} (mT) \left(\frac{T}{m} \right)^{\frac{1}{4}}, \quad (14)$$

where $n(z, T)$ is the local density of positrons at distance z from the nugget's surface, which has been computed in the mean field approximation in [36] and has the following form

$$n(z, T) = \frac{T}{2\pi\alpha} \frac{1}{(z + \bar{z})^2}, \quad \bar{z}^{-1} \approx \sqrt{2\pi\alpha} \cdot m \cdot \left(\frac{T}{m} \right)^{\frac{1}{4}}, \quad (15)$$

where \bar{z} is the integration constant is chosen to match the Boltzmann regime at sufficiently large $z \gg \bar{z}$. Numerical studies [38] support the approximate analytical expression (15).

Numerically, the number of weakly bound positrons can be estimated from (14) as follows:

$$Q \approx 3 \cdot 10^{11} \left(\frac{T}{20 \text{ keV}} \right)^{\frac{5}{4}} \left(\frac{R}{2.25 \cdot 10^{-5} \text{ cm}} \right)^2. \quad (16)$$

These positrons from electrosphere being in the equilibrium (when the AQN experiences a relatively small annihilation rate in dilute galactic environment) will normally occupy very thin layer around the AQN's quark core as computed in [36, 38]. However, in our case when the AQN enters the Earth's atmosphere a large number of non-equilibrium processes (such as generation of the shock wave resulting from large Mach number) are expected to occur. In what follows we assume that, to first order, that the finite portion of positrons $\sim Q$ leave the system as a result of the complicated processes mentioned above, in which case the AQN as a system acquires a negative electric charge $\sim -|e|Q$ and get partially ionized as a macroscopically large object of mass $M \simeq m_p B$. The ratio $eQ/M \sim 10^{-14} e/m_p$ characterizing this object is very tiny. However, the charge Q itself is sufficiently large being capable to attract the positively charged ions from air (for example during the thunderstorm).

2.3. AQN spallation

One more feature of the AQN propagating in Earth's atmosphere (which plays an important role for the present work) is as follows. As mentioned in Sect.2.1 the AQN is absolutely stable object because the energy per unit baryon charge in CS phase (AQN's core) is smaller than for nucleons. However, some external strong impact and large energy injection (due to sudden annihilation events within the AQN's quark core) may disintegrate AQN when a small chunk from the original AQN material (in form of the anti-quark-matter) is separated from the original parent AQN. In a sense, it is very similar to well known and well studied spallation effect which is very common phenomenon in nuclear physics. We coin the corresponding secondary particles as AQN_s, where subscript s stands for secondary particle or spallation.

The secondary AQN_s are obviously not absolutely stable objects as the key element for the stability, the axion domain wall with its QCD substructure, see Fig.1, cannot remain in the system after spallation. This should be contrasted with conventional spallation effect in nuclear physics when both, the original nucleus and the secondary particles are absolutely stable objects (with respect to strong interactions) as they both propagate in the same hadronic (low chemical potential, low temperature) phase³, while AQN's core is assumed to be in CS phase characterized by sufficiently large chemical potential (large pressure), see phase diagram in ref. [25].

The secondary AQN_s could be much smaller in size than AQN. The corresponding fragment really represents very small chunk of the original (anti-matter) material. As we discuss in next Sect.3 the secondary AQN_s will be identified with BL events as conjecture (17) states. Precisely these chunks of antimatter material will play the role of engines powering the BL dynamics in this proposal. These objects should have typical sizes $B_{\text{AQN}_s} \approx 10^{15}$ (to be discussed below), which is 10 orders of magnitude smaller than original AQN with typical baryon charge $B \approx 10^{25}$.

In our discussions which follow we assume that the spallation is likely to occur as the most important ingredient required for spallation, a high fraction of ionized particles in surrounding area, is present during the thunderstorms. As we discuss below, the highly ionized environment dramatically increases the effective strength of interaction of the AQN with surrounding material expressed by parameter κ in (13), which drastically increases the internal temperature leading to spallation, see Sect. 3.2 with more comments on this matter. The spallation dynamics, the size distribution of the secondary AQN_s and other related questions have not been worked out yet (detail discussions on formation mechanism for original AQN can be found in ref. [25]). The corresponding questions are well beyond the scope of the present work. We take

³The secondary AQN_s can be thought as the metastable states, similar to supercooled or superheated liquid droplets when large chunk of matter suddenly appears in a "wrong" environment (temperature and pressure) not supporting its phase.

agnostic view in this work on spallation dynamics. We just assume that the spallation occurs and we use a typical size (or what is the same, the baryon charge) of the secondary AQN_s to fit the BL observations. This is the only input parameter to be used in the present work, while all other observables relevant for BL physics will be derived from this single input parameter.

To conclude this overview section on AQN framework one should mention here that this model with the same set of parameters to be used in the present work may explain a number of puzzling and mysterious observations which cannot be understood as conventional astrophysical phenomena. In particular, there are many mysterious observations which occur at dramatically different scales at very different cosmological eras, which also might be related to AQN-induced phenomena. It includes BBN epoch, dark ages, as well as galactic and Solar environments. It also includes a number of puzzling and mysterious CR-like events which could be also related to AQN-induced phenomena, see concluding sections 6.1 and 6.3 for the details and references.

3. Proposal (17) confronts the observations

Our proposal can be formulated as follows. The secondary particles (after spallation) in form of the antimatter AQN_s are identified with Ball Lightning events, i.e.

$$\text{secondary AQN}_s \text{ events} \equiv \text{Ball Lightning events.} \quad (17)$$

The main goal of this section is to argue that the various of observations as formulated in Introduction 1 collected for decades can be naturally explained (though very often on a qualitative level) if one accepts the proposal (17).

3.1. Source of the energy powering BL

The source of the energy in the AQN framework is obviously the antimatter annihilation with surrounding material. Every annihilation event of a single baryon produces approximately 2 GeV energy. We fix the basic parameter of the proposal (17) by fixing the total amount of antimatter in form of the secondary AQN_s. According to (1) the typical energy for BL events vary from 1 kJ to 10³ kJ. The mean energy for BL is estimated in [2] as 2 · 10² kJ. To simplify our estimates below we use 10² kJ as a typical average energy for BL events. Therefore, we fix the amount of antimatter hidden in form of the AQN_s accordingly:

$$10^2 \text{ kJ} \approx 10^{15} \text{ GeV} \quad \rightarrow \quad B_{\text{AQN}_s} \approx 10^{15}, \quad R_{\text{AQN}_s} \approx \left(\frac{B_{\text{AQN}_s}}{B} \right)^{\frac{1}{3}} R \approx 10^{-8} \text{ cm} \quad (18)$$

where we use conversion factor $J = 0.6 \cdot 10^{10} \text{ GeV}$. One should emphasize that the chunks of the AQN_s could have very different sizes. Therefore, a wide window for the BL energy distribution (as extracted from observations, see Fig 5 in [2]) could be easily accommodated in our proposal (17) to fit the data. However, we stick with the average value (18) in what follows for simplicity our qualitative analysis. One should also add that a large variation in energies of the BL events (1) strongly suggest that the source of the energy is unlikely to be related to any fundamental subatomic particles when one should expect a similarities for different events. In contrast, the proposal (17) is based on complex classical macroscopical system with variety of sizes which is perfectly consistent with broad distribution of the energy scales (1).

3.2. BL is electrically charged

Now we want to argue that AQN_s will carry the electric charge Q_{AQN_s} after spallation. The corresponding numerical value can be easily estimated by assuming that the internal temperature after spallation remain the same as for original AQN (16). Therefore, one can use the rescaling to arrive to the estimate:

$$\frac{Q_{\text{AQN}_s}}{Q} \approx \left(\frac{B_{\text{AQN}_s}}{B} \right)^{\frac{2}{3}} \approx \left(\frac{10^{15}}{10^{25}} \right)^{\frac{2}{3}} \approx 2 \cdot 10^{-7} \quad \rightarrow \quad Q_{\text{AQN}_s} \approx 6 \cdot 10^4, \quad (19)$$

where we used the feature that the Q charge is the surface effect, while the baryon B charge is the volume effect. The presence of the charge in the system will play a key role in the dynamics to be discussed below. First of all, presence of the charge Q in the system in the original AQN implies that the AQN can attract the positively charged ions from the air such that the rate of annihilation may dramatically increase. This effect can be described by drastic increase of the phenomenological coefficient κ in (11) such that effective temperature T also suddenly increases when AQN enters the region of a highly ionized gas. As a consequence, the spallation phenomenon may be much more efficient (and likely to occur) in this case.

The presence of large density of ionized particles in air is known to occur during the thunderstorms in thunderclouds (even without strikes). Therefore, the association of the BL with thunderstorms, see item (i) from Sect.1.1, has its direct explanation within our proposal due to a sudden and dramatic increase of κ (and corresponding internal temperature T) as mentioned above. These dramatic changes may lead to spallation effect which consequently results in formation of the secondary particles AQN_s which are identified with BL according to (17).

Furthermore, the secondary particles AQN_s are also charged according to (19). One should emphasize that this estimate for Q_{AQN_s} refers to the internal (bound) charge which are localized very close to the quark core with size (18). The induced charge due to other processes, see below could be much greater. The presence of the electric charge in the system is also consistent with observations which suggest that BL gets attracted (due to the induced charges) to the metallic surfaces, wires, antennas [2, 4].

3.3. Spectral properties of the BL radiation. Size of BL(in visible frequency bands).

The spectral properties of the AQN emission has been studied previously as reviewed in Appendix A. The key feature of this radiation is very broad spectrum (in contrast with black body radiation) up to cutoff frequency which occurs around $\omega \approx T$. What happens to these keV photons emitted by the AQN_s (identified with BL) with internal core temperature $T \approx 6$ keV according to (40)?

The dominant mechanism of absorption for such energetic X rays is the atomic photoelectric effect, see Fig 33.15 for $Z = 6$ (Carbon) in PDG [39]. For the Oxygen ($Z=8$) and Nitrogen ($Z=7$) the effect is slightly higher due to very strong dependence on Z [40]:

$$\sigma_{\text{photo-effect}} \approx \frac{32\sqrt{2}\pi}{3} r_0^2 Z^5 \alpha^4 \left(\frac{m}{\omega}\right)^{\frac{7}{2}}, \quad r_0 \equiv \frac{\alpha^2}{m^2} = 2.8 \cdot 10^{-13} \text{cm}. \quad (20)$$

Based on this cross section the mean free path λ for 6 keV photons can be estimated as

$$\lambda^{O,N}(6 \text{ keV}) \approx 10 \text{ cm}, \quad [\text{to be identified with visible size of BL}]. \quad (21)$$

where we used experimental data for $Z = 6$ (Carbon), see Fig 33.19 and rescaled for the Oxygen ($Z=8$) and Nitrogen ($Z=7$).

The atomic photoelectric effect is accompanied by electron emission. The life time of a free electron in air is very short, around $0.1\mu\text{s}$, see e.g. [41] such that free electron will be quickly absorbed by atoms in air on very short distances around 10^{-4}m , much shorter than (21). These excited and ionized atoms and molecules (made of Oxygen and Nitrogen along with many other elements from soil) will emit visible light which is observed as radiation coming from BL according to our proposal (17). Therefore, we identify the size of BL (in visible frequency bands) with mean free path λ as stated in (21). This scale is perfectly consistent with observations (3).

Few comments are in order:

1. The mean free path λ introduced above is highly sensitive to the frequency of radiation (or what is the same, the internal temperature). Therefore, even a minor variation in internal temperature of the AQN_s can dramatically modify the mean free path. To illustrate this feature we estimate λ for 10 keV photons:

$$\lambda^{O,N}(10 \text{ keV}) \approx 70 \text{ cm}, \quad [\text{to be identified with visible size of BL}] \quad (22)$$

Our main point with this illustration is that the visible size of the BL in this proposal (17), being identified with λ , is not related to a basic energetic characteristic (1) which could dramatically vary (three

orders of magnitude or more) from one event to another. Rather, the variation in size of the BL is related to very small variation in internal temperature T ;

2. This picture of emission of the visible light is consistent with observation that average density of BL is the same as average density of the surrounding air because the quark matter core with $M_{\text{AQNs}} \approx 10^{-9}\text{g}$ is negligible in comparison with weight of air in volume λ^3 . The observed visible light from BL in this proposal is obviously not related to hot plasma, nor to convective behaviour of a hot gas, see (item iv) from Sect.1.1. This proposal also naturally explains the observation that BL normally moves horizontally as the average density of the BL object is the same as the air density at the same temperature⁴;

3. This picture of emission of the visible light is consistent with observation that the spectrum contains soil components (Si I, Fe I, Ca I) (item x) from Sect.1.1. This is because the soil components have much larger Z (and therefore, the cross section (20) is much greater). As a result, even a tiny amount of these components in air (e.g. in form of the dust particles) could generate very strong intensity lines associated with these elements, which is consistent with observations [11, 12];

4. From the estimate (21) of BL size in the visible frequency bands one can estimate the average energy density for our specific parameters (18) for BL propagating in air as follows:

$$\epsilon^{\text{O,N}} \equiv \frac{(B_{\text{AQNs}} \cdot m_{\text{p}})}{(\lambda^{\text{O,N}})^2 \bar{L}} \approx \frac{10^2 \text{kJ}}{(10 \text{ cm})^2 \cdot (40 \text{ m})} \approx 0.25 \frac{\text{J}}{\text{cm}^3}, \quad \bar{L} \approx \bar{v}_{\text{BL}} \cdot \tau \approx 40 \text{ m}, \quad (23)$$

where \bar{L} is an average length for BL's path with parameters from (4). This estimate is consistent with value (2) extracted from observations in visible frequency bands;

5. This picture of emission is consistent with observation that BL emits UV or x ray radiation along with visible light as discussed above. In fact, UV and x rays are originated from the the core of the AQNs , in contrast with visible light which is a secondary process in the AQN framework as described above. This picture is perfectly consistent with (item xi) from Sect.1.1 when the presence of UV or x rays from BL had been directly observed [13]. The presence of the UV or x rays from BL is also supported our estimate for the total power of emission which suggests that the power in visible light represents only a small fraction of the total power, see next Sect. 3.4;

6. Annihilation of the baryons is always accompanied by annihilation of the electrons from atoms with positrons from AQN's electrosphere. The corresponding total energy injection per single event (MeV scale) due to e^+e^- annihilation is negligible ($\sim 10^{-3}$) in comparison with GeV scale due to hadron's annihilations. However the emission of the 0.511 MeV photons from e^+e^- annihilation may play a crucial role in understanding of items viii and xi from Sect.1.1. This is because the mean free path for such energetic photons in air is very large, $\lambda(0.5 \text{ MeV}) \sim 10 \text{ m}$ such that these photons can ionize the surrounding space and could be responsible for ionizing radiation. A number of observed phenomena which could be related to ionizing radiation from BL were reported in [3].

3.4. BL life time. The power of radiation. The BL's internal size.

The internal size of quark matter of the AQNs is determined by the quark matter core $R \approx 10^{-8}\text{cm}$ from (18). However, the effective size of the quark matter material with surrounding positrons is dramatically larger than quark matter core itself (similar to atoms with typical size $a \approx 10^{-8}\text{cm}$ being much larger than the size of a nuclei $\sim 10^{-13}\text{cm}$).

We define the effective radius R_{eff} as the scale where positrons from electrosphere remain to be strongly bound to the quark's core at the internal temperature $T \approx 6 \text{ keV}$. The corresponding scale can be estimated from the condition that the binding energy of the positrons is approximately equal to internal temperature

⁴The description of the spectrum in terms of very high temperature $T \sim 10^4\text{K}$ as presented in [11, 12], see next item 3, is a matter of convenience to describe a highly ionized system. In fact there is no real temperature in the system as there is no thermal equilibrium when the temperature could be defined in the system. The thermal equilibrium is obviously cannot be achieved in BL system. The same comment obviously applies to the lightning phenomenon as it is a highly non- equilibrium processes. The black body radiation which normally characterizes the system being in the thermal equilibrium is not present in data [11, 12]. The eyewitness also suggest that there is no any heat associated with BL [2-4].

$T \approx 6$ keV. This gives $R_{\text{eff}} \approx 10^{-6}$ cm, see (41) in Appendix A for numerical estimates. The corresponding scale should be treated as internal structure of the system, in contrast with the scales (21) and (28) which should be treated as environment-dependent scales.

The significance of the scale R_{eff} is related to the fact that this scale determines the rate of the antimatter annihilation (and therefore BL's life time in the AQN framework) hidden in form of the AQN_s . To be more precise, the rate of annihilation of the baryon charge due to head on collisions of the air molecules with anti-matter AQN_s can be estimated as follows:

$$\frac{dB}{dt} \approx -(\pi R_{\text{eff}}^2) \cdot n_{\text{air}} \cdot v_{\text{air}}, \quad (24)$$

where we assume that the successful annihilation events represent a finite fraction of order one for all collisions. Another finite fraction of collisions are elastic scattering events when molecules of air scatter without annihilation. In formula (24) we take a typical density of surrounding baryons as $n_{\text{air}} \simeq 30 \cdot N_m \simeq 10^{21} \text{ cm}^{-3}$, with $N_m \simeq 2.7 \cdot 10^{19} \text{ cm}^{-3}$ being the molecular density in atmosphere when each molecule contains approximately 30 baryons. The rate of annihilation as given by expression (24) in all respects is similar in spirit to the right hand side of eq. (11) in our estimation for the energy injection rate for the AQN when it just enters the earth's atmosphere.

The v_{air} (typical velocity of molecules in air) can be estimated from condition

$$\frac{m_{\text{air}} v_{\text{air}}^2}{2} \approx \frac{3}{2} T_{\text{air}} \rightarrow v_{\text{air}} \approx 5 \cdot 10^4 \frac{\text{cm}}{\text{s}}, \quad (25)$$

where $T_{\text{air}} \approx 300\text{K}$ is air temperature. Collecting all the numerical factors together we arrive to estimate:

$$\frac{1}{B_0} \frac{dB(t)}{dt} \approx -\frac{1}{B_0} \frac{1.5 \cdot 10^{14} \text{ baryons}}{\text{s}} \left(\frac{R_{\text{eff}}}{10^{-6} \text{ cm}} \right)^2 \approx -\frac{1}{\tau}, \quad \tau \approx 6.7\text{s} \quad (26)$$

where we inserted B_0^{-1} for normalization with $B_0 = B(t=0)$ being defined as initial (anti)baryon charge of the AQN_s with its effective radius as estimated in (41). In reality the time scale (26) for our benchmark value for B_0 as given by (18) is slightly longer as we ignored in our numerical estimates the elastically scattered events (which obviously decrease the rate (24) and consequently increase the estimate for τ) as mentioned above. Few comments are in order:

1. The time scale which appears in (26) is perfectly consistent with observations according to (4). This is a highly nontrivial consistency check for entire proposal (17) because two observed parameters (total energy of the BL (18) and its life time (26)) are unambiguously connected in this proposal. It is very hard to imagine any other mechanism when these two very different entities are tightly connected and agreed with observed values;
2. The power of radiation (total power) can be estimated as

$$P_{\text{tot}} \approx \frac{B_{\text{AQNs}} \cdot m_p}{\tau} \approx \frac{10^2 \text{ kJ}}{\tau} \approx 10 \text{ kW}, \quad (27)$$

which is consistent with (5) extracted from studies in the visible frequency bands. Our estimate (27) suggests that the emission in visible light could be only a small fraction of the total power generated by BL;

3. Formula (26) holds as long as portion $f(t) \equiv B(t)/B_0$ represents a finite fraction of the initial baryon charge of order one. This is because for very small $f(t) \ll 1$ some dramatic changes in rate of annihilation may occur which consequently may result in explosion instead of smooth and slow decay determined by the time scale τ , see next comment. This behaviour is consistent with item (v) from the list in Sect.1.1;

4. The explosion occurs if the the annihilation rate (26) suddenly increases due to some external impacts or as a result of successful simultaneous annihilation of a large number of baryons from air when internal temperature must instantaneously increase to equilibrate heating and cooling processes. In this case the time scale (26) suddenly and dramatically decreases resulting in very intense flash of broad band radiation and consequent formation of an acoustic shock wave. This would appear as an explosion of BL when all

remaining antimatter in the AQN_s get annihilated at once. The properties of the resulted shock wave are different from conventional chemical or nuclear explosions but similar to the ones studied in [31];

5. The size of the BL in visible bands during a smooth evolution in this framework is determined by the photon's mean-free path as explained in Sect. 3.3. This scale is not very sensitive to a slow decreasing of the (anti)baryon charge in the quark core during the BL evolution, as it is determined by (almost) constant internal temperature T according to formula (40) from Appendix A. This conclusion is in agreement with observations from item (ii) from the list in Sect.1.1.

3.5. BL passing through glass windows. The BL's new scale of the problem.

The authors of ref. [10] with a help of optical and scanning microscopes and laser beam probing the glass, have found the traces which are left by 20 cm BL passing through the window glass. The authors discovered a cavity of 0.24 mm diameter, see Fig.3 in that paper. The authors correctly interpreted this event as an undeniable evidence of a "material" nature of BL. The scale of this cavity is dramatically different from the 20 cm scale of the BL as observed at visible frequency bands.

In the AQN framework the emergence of this new scale (0.24 mm in comparison with 20 cm scale as observed in visible light) has a very natural explanation. Indeed, the mean free path for a similar energy photons in Si (12 keV in Si instead of 6 keV in air, see relevant comment in footnote⁵) is dramatically shorter in comparison with O and N atoms from air. It can be extracted from the same Fig 33.19 from PDG [39] which gives the following estimate:

$$\lambda^{\text{Si}}(12 \text{ keV}) \approx 0.25 \text{ mm}, \quad [\text{to be identified with size of a cavity in glass}] \quad (28)$$

where we use $\rho(\text{Si}) = 2.3\text{g}/\text{cm}^3$ for the estimate. The estimate (28) is very instructive as it shows a dramatic difference between two scales (21) and (28). A proper computation of the internal temperature (and corresponding photon's energy) entering the estimate (28) is very hard technical problem, see footnote 5. However, our generic claim that the scale (28) must be dramatically smaller than the scale (21) is a solid qualitative prediction of the framework as it is entirely determined by the differences in photon's mean free paths for two very different environments with similar x-rays energies. The estimate (28) shows the consistency of the entire framework when the scale of the BL phenomena is determined by the interaction of the AQN_s core with environment, rather than by its internal structure. As we discussed in previous Sect. 3.4 the internal size of the AQN_s core is dramatically smaller than scale (28).

The energy density injected at the instant when BL passing through the window glass of width $l \approx 2\text{mm}$ can be estimated from (28) as follows:

$$\epsilon^{\text{Si}} \equiv \frac{(\Delta B_{\text{AQN}_s} \cdot m_p)}{(\lambda^{\text{Si}})^2 l} \approx \frac{10^2 J}{(0.25 \text{ mm})^2 (2 \text{ mm})} \approx 10^3 \frac{\text{kJ}}{\text{cm}^3}, \quad \Delta B_{\text{AQN}_s} = (\pi R_{\text{eff}}^2 l) \cdot n_{\text{glass}} \approx 10^{-3} B_{\text{AQN}_s}, \quad (29)$$

where ΔB_{AQN_s} is amount of antimatter being annihilated during BL's passage through the window glass of width $l \approx 2\text{mm}$. In this estimate we use the same $R_{\text{eff}} \approx 10^{-6}\text{cm}$ which enters (24) from previous Sect. 3.4. For numerical estimates we use the baryon number density of glass $n_{\text{glass}} = \rho_{\text{glass}}/m_p \approx 1.4 \cdot 10^{24}\text{cm}^{-3}$.

Important point here is that ϵ^{Si} is dramatically greater than a similar estimate for BL propagating in air as given by (23). This enormous energy density is obviously more than sufficient to melt the glass in small volume of size $(\lambda^{\text{Si}})^2 l$. The process of the glass melting in the AQN framework can be thought as (almost) instantaneous event when the 12 keV photons radiate along AQN_s path with area of size $(\lambda^{\text{Si}})^2$

⁵Precise estimation of the internal temperature when the AQN_s crosses the interface between very different environments is very difficult technical problem. In particular, the internal temperature obviously should increase in comparison with temperature in air (40) when the interface is crossed. However, the computation of this increase is hard to carry out. In particular, the thermal equilibration in the AQN_s electrosphere for this short passage of the interface is unlikely to hold, which obviously complicates the problem. We account for this and related effects by increasing the effective temperature from 6 keV to 12 keV which appears in (28) to fit the observed value. A proper procedure to account for this and related effects is to solve the problem for the AQN_s dynamics when it crosses the interface between air and glass which are characterized by dramatically different densities and atomic compositions. The corresponding computation is well beyond the scope of the present work.

and length l . This (almost) instant process ends after AQN_s passes through glass windows on time scale $l/v_{BL} \approx 0.5\text{ms}$, after which BL returns to its previous original size 20 cm observed for BL propagating in air. Such short changes in size in time scale of order 0.5ms of course cannot be noticed by a human eye (the threshold is about 20 ms). In fact all witnesses report that no any changes occur during the course of BL passing through glass windows. Few comments are in order:

1. In the AQN framework the BL passing through glass windows (or any other surfaces) is a very natural effect. Indeed, the available energy density of the BL crossing a solid material could be very large according to (29). When the BL crosses the window the emitted (from AQN_s core) photons will be localized on a scale of order (28). As a result of this “focusing” effect the energy density assumes enormous value (29) in form of a very short pulse with time scale of order 0.5ms. This enormous energy density is sufficient to melt essentially any material;
2. This picture of passing BL through the window is consistent with studies of ref. [10] where “one can assume that the heating of the glass was carried out by a powerful pulse of electromagnetic radiation” (it is a direct quote);
3. The emergent scale of the problem (28) is not related in anyway to the internal structure of the BL itself which was discussed in previous Sect. 3.4. Rather, the scale (28) emerges due to interaction of the AQN_s with environment (window glass) where the mean free path λ^{Si} is relatively short. It should be contrasted with our discussions of propagation of BL in air in Sect. 3.3 where dramatically different scale (21) emerges.

3.6. How does BL emerge (in form of the AQN_s) after spallation?

As we mentioned in Sect. 2.3 the parent AQN may disintegrate (as a result of some external impacts, see below) when one or several smaller pieces consisting the original AQN material (in form of the anti-quark-matter) get separated. The phenomenon in many respects is similar to well known process in nuclear physics. We coined the corresponding secondary particles as AQN_s and identify them with BL (17). As we mentioned previously, the spallation effect may become highly efficient during the thunderstorms in thunderclouds (even without strikes) due to presence of large density of ionized particles and dramatic increase of the annihilation rate which consequently results in sudden increase of the internal temperature T . Therefore, the association of the BL with thunderstorms characterized by high density of ionized particles, has its natural (though very qualitative) explanation within our proposal.

The AQN itself represents the DM macroscopical object which enters the Earth’s atmosphere with typical velocity $v_{AQN} \sim 10^{-3}c$. It may cross the Earth by losing only tiny portion of the momentum and antimatter material along its path due to a very large baryon number $B \approx 10^{25}$ carried by the system, as reviewed in Sect.2.1. The situation with the secondary AQN_s is dramatically different because of its much smaller baryon charge $B_s \approx 10^{15}$ in which case a complete annihilation of the antimatter material in atmosphere (or earth’s surface) becomes inevitable.

The question we address in this subsection is as follows. How long does it take for AQN_s to slow down from typical velocity $10^{-3}c$ to essentially zero velocity at the earth’s surface when BL is normally observed? To estimate the corresponding length scale L (when stopping occurs) we observe that the elastic head-on collision of AQN_s with a single baryon charge leads to decrease of the initial AQN_s momentum by amount $\sim 2m_p 10^{-3}c$. In case of annihilation or non-head on collision the decrease of momentum is numerically smaller. However, for a simple estimation we can assume that the amount of material from air in a cylinder of radius R_{eff} , and length L must be the same order of magnitude as the baryon charge $B_s \approx 10^{15}$ for the AQN_s to lose its huge initial velocity, i.e.

$$B_s \sim (\pi R_{\text{eff}}^2) \cdot n_{\text{air}} \cdot L \quad \rightarrow \quad L \sim 3 \text{ km}, \quad (30)$$

where $R_{\text{eff}} \approx 10^{-6}\text{cm}$ is the internal effective size of the AQN_s which has been used previously in Sect. 3.4. Few comments are in order:

1. We consider the numerical value for L to be a very reasonable estimate. Indeed, the scale (30) corresponds to a typical size of the thunderclouds. Therefore, the AQN_s can reach the earth’s surface after spallation in thunderclouds by losing its huge original velocity to become BL with very low velocity at the surface

where it is normally observed. A typical stoppage time τ_s , when AQN_s loses its 99% of its momentum, can be estimated as $\tau_s \approx 2$ s which is slightly shorter than BL's life time τ from (26). At this velocity the BL becomes observable in visible frequency bands. A quantitative estimate for this stoppage time $\tau_s \approx 2$ s is given in Appendix B;

2. One can explicitly see that very small AQN_s with $B_s \ll 10^{15}$ cannot survive a several kilometres journey from thunderclouds to the earth's surface as they get completely annihilated long before they reach the surface. This could be a simple explanation (within AQN framework) for the well established feature that BL has a lower energetic bound (1). In the AQN framework this bound emerges as a result of identification (17) when two entities (energy E_{BL} and baryon charge B_s) are tightly linked in our proposal: $E_{BL} \approx B_s(2\text{GeV})$;
3. The estimate (30) also shows why extremely large $B_s \gg 10^{15}$ have never been observed as BL events. Indeed, the observed maximum for E_{max} is, at most, two orders of magnitude above the average value according to (1). In the AQN framework this feature is explained as follows. Very large values of $B_s \gg 10^{15}$ imply that the stoppage distance L must be much longer in comparison with our estimate (30). Therefore, the secondary AQN_s with very large $B_s \gg 10^{15}$, if they are formed, will hit the earth's surface with very high velocities and get completely annihilated only in deep underground regions, in contrast with BL which assume very low velocity near the surface. As a result, such energetic events with $B_s \gg 10^{15}$ are less likely to be observed in comparison with typical BL⁶;
4. One should emphasize that the spallation is not a mechanism of production of anti-quark material powering BL. Antiquark nuggets had been produced during the QCD transition in early Universe and survived until present epoch, as reviewed in Sect. 2.1. Spallation is a secondary phenomenon when small portion of this anti-quark material disintegrated from the original anti-matter AQN. In other words, spallation is not a production of engine powering the BL. Rather, this engine in form of the antimatter (we observed today in form of BL) had been produced during the QCD transition in early Universe.

3.7. Summary. Consistency of the proposal (17) with observed features from Sect.1.1

In subsections 3.1-3.6 above we argued that our proposal (17) is perfectly consistent with observed items from Sect.1.1. However, all our explanations and estimates were scattered in the text. The goal here, for consistency and uniformity of presentation, is to summarize and collect all of the items in the same order, one by one with a precise reference to a specific and detail estimate given in the text. The observed features from Sect.1.1 include:

- (i) BL's association with thunderstorm is discussed in Sects. 3.2 and 3.6 with specific estimate (30) of a distance BL propagates from thunderclouds where it was formed to the surface where it is normally observed. The basic reason for thunderclouds to play a key role in BL formation is the generation of the AQN's internal negative electric charge which dramatically increases the interaction with positively charged ions from surrounding area during thunderstorms;
- (ii) Typical size of BL in the visible frequency bands is discussed in Sect. 3.3 with specific estimates as given by (22) and (21). Lifetime of BL is discussed in Sect. 3.4 with specific estimate for τ as given by (26). The arguments suggesting that there should be no strong time-variation of these parameters throughout the BL's time evolution is presented in item 4 in Sect. 3.4;
- (iii) Most of BL events are likely to occur in open air as BLs (in the AQN framework) propagate to earth's surface from thunderclouds. However, BL can easily cross a glass or any other material and continue to propagate in enclosed spaces such as buildings or aircraft, see Sect. 3.5 with corresponding discussions and estimation for the cavity size for glass (28). Similar estimates are applicable for any other materials, including metals in case of an aircraft;
- (iv) Average density of the BL is the same as surrounding air, see item 2 in Sect. 3.3. This is because the observed radiation from BL is not associated in any way with heating of the air inside the visible part of BL. The emission in visible frequency bands from BL has dramatically different nature as explained in details in Sect. 3.3 with specific estimation (21) of the visible portion of BL;

⁶In fact, there are many recorded events, which are classified as "Pseudo-meteorites events" when a meteor-like event is observed, but no actual physical meteorite is found in the area, see 5.1 for references and details.

- (v) A typical lifetime of BL is discussed in Sect. 3.4 with specific estimate for τ as given by (26). This estimate assumes a smooth evolution. In some cases (resulting from some external impacts) the explosion may occur as mentioned in item 3 in Sect. 3.4;
- (vi) In case of a still evolution the lifetime is determined by formula (26) from Sect. 3.4. This formula holds for smooth propagation of BL in air when its entire original energy is released in steady way in form of the x rays and visible light without much damage to surrounding area;
- (vii) The process of BL crossing through metal screens or glass is described in Sect.3.5 with specific estimate (28) for size of a cavity in glass as a result of such passage. A typical time for such passage is estimated on the level of 0.5 ms such that this fast variation in BL's size cannot be noticed by a human eye;
- (viii) The radiation from the AQN_s is very broad band in nature. In particular, it includes MeV photons along with x rays, see item 6 in Sect. 3.3. Furthermore, the AQN_s carries internal negative charge which could be much larger in value than original initial charge (19) after spallation. The atomic photo-effects described in Sect. 3.3 may also ionize surrounding air. All these phenomena may produce a number of effects described in (viii), including acrid odors and others phenomena due to ionizing radiation as reported in [3];
- (ix) In the AQN framework the emergence of this new scale (0.24 mm) as reported in ref. [10] can be naturally explained, see Sect. 3.5. The main point is that the scale (28) emerges due to interaction of the AQN_s with environment (window glass). This new scale is not related to the internal structure of the BL;
- (x) the spectrum contains soil components (Si I, Fe I, Ca I) according to [11, 12]. This is because the soil components have much larger Z such that the cross section (20) is much greater than for dominant air components O and N. As a result, even a tiny amount of these soil components in air could produce strong intensity lines associated with these elements, see item 3 in Sect.3.3;
- (xi) The direct observations explicitly show [13] that the spectrum from BL must include UV or/and x ray emission. This observation is perfectly consistent with the picture of emission advocated in this work, see items 5 and 6 from Sect. Sect.3.3.

3.8. Concluding comments on proposal (17)

We conclude this section with the following very generic comments. The AQN model was suggested long ago to resolve some fundamental problems in cosmology, see Sect.2. The corresponding AQN parameters (including spectral properties of radiation, etc) were also worked out long ago to address many puzzles and mysteries mostly related to observed excesses of radiation at different frequencies bands at different cosmological and astrophysical scales, see Sect.6.3 for a brief review. The AQN model was not designed to address the BL physics. In our estimates in this work we use exactly the same set of parameters extracted from our cosmological studies to test bold unorthodox proposal (17) relating the BL and DM physics.

We produced a number of estimates relating the observed BL parameters listed in Sect. 1.1 with AQN parameters. All our estimates in this section are based on a single input parameter (18), the baryon charge (or what is the same, the energy of BL) of the AQN_s identified with BL according to the proposal (17). In particular, the visible size of BL (21), its typical life time (26), the cavity size (28) are determined by incorporating this single input normalization parameter (18) with variety of well known physical observables, such as photo-effect cross section for different atoms, the density of the environment, mean free paths, etc.

It is a highly nontrivial consistency check that all our estimates of the BL characteristics in this section assume very reasonable values being consistent with observations relating BL and DM physics in AQN framework. Indeed, the rate of annihilation determines the internal temperature of the AQN_s according to (40), which consequently determines the spectrum, which (through the atomic photo-effect) determines the mean free path and the size of the BL in visible frequency bands (21) in air. The same parameters determine the life time of the BL according to (26). It strongly supports the basic idea formulated as (17) that the anti-matter nuggets, representing the DM objects in empty space, in fact become the engines powering the BL physics and producing profound effects when these objects enter the earth's atmosphere.

This consistency check in fact extends to the next Sect 4 where we demonstrate that the frequency of appearance of BL is consistent with flux of DM objects in form of the AQNs. In this case the basic normalization factor is the dark matter density $\rho_{DM} = 0.3 \text{ GeV} \cdot \text{cm}^{-3}$ extracted from numerous cosmological

studies. It turns out that precisely this factor ρ_{DM} determines the frequency of appearance of BL, which further strengthens the proposal (17) relating BL and DM physics.

4. Frequency of appearance

We start with overview of the recent analysis [8, 42] for frequency of BL appearance. The corresponding lower bound flux has been estimated as [8]:

$$\frac{d\Phi_{\text{BL}}}{dA d\Omega} > 1.75 \cdot 10^{-24} \frac{\text{events}}{\text{cm}^2 \cdot \text{sr} \cdot \text{s}}. \quad (31)$$

The author of ref. [8] argues that the actual frequency of BL is in fact much greater than lower bound (31). However, it is hard to estimate. We would like to represent the lower bound (31) using more appropriate (for rare events) units

$$\frac{d\Phi_{\text{BL}}}{dA} > 4 \cdot 10^{-6} \frac{\text{events}}{\text{km}^2 \cdot \text{yr}}, \quad (32)$$

where we insert factor 2π into (32) as the solid angle to account for all directions from entire sky. One can formulate the following question. It is known that BL are associated with lightning, see item (i) in Sect. 1.1. Therefore, one can argue that the lightning should play an important role in formation of the BL⁷. Then, why the rate (32) is much lower than an average frequency of conventional lightnings in the continental U. S., which is about $24 \text{ km}^{-2} \text{ yr}^{-1}$? We rephrase the same question in a different way: what is so special about very rare lightning events which produce BL (32) in comparison with vast majority of lightning events which do not lead to BL?

Now we turn to another side of our story, the Dark Matter. In the AQN framework the corresponding AQN flux is proportional to the dark matter number density $n_{\text{DM}} \propto \rho_{\text{DM}}/\langle B \rangle$. It is convenient to represent the DM flux as given by (8) and (9) as follows:

$$\frac{d\Phi}{dA} = \frac{\Phi}{4\pi R_{\oplus}^2} = 4 \cdot 10^{-2} \left(\frac{\rho_{\text{DM}}}{0.3 \text{ GeV cm}^{-3}} \right) \left(\frac{v_{\text{AQN}}}{220 \text{ km s}^{-1}} \right) \left(\frac{10^{25}}{\langle B \rangle} \right) \frac{\text{events}}{\text{yr} \cdot \text{km}^2}, \quad (33)$$

where we assumed the standard halo model with the local dark matter density being $\rho_{\text{DM}} \simeq 0.3 \text{ GeV cm}^{-3}$ and canonical galactic wind $v_{\text{AQN}} \simeq 220 \text{ km s}^{-1}$. The number density of the AQNs is very tiny: $n_{\text{AQN}} \simeq \left(\frac{\rho_{\text{DM}}}{m_p \langle B \rangle} \right)$ as it is suppressed by factor B^{-1} . This should be contrasted with canonical type of WIMPs with typical mass $\sim 10^2 \text{ GeV}$ in comparison with AQN mass $\sim 10^{25} \text{ GeV}$. Conventional DM detectors designed for WIMP searches are obviously useless to study the DM in form of the AQNs as there will be no any events for million of years. The Cosmic-Ray (CR) labs, on other hand, may record the AQN-induced events, and we shall comment on this with relation to recording some unusual CR-like events during the thunderstorms in Sect. 6.1.

Now we are ready to estimate the flux for BL within AQN framework when AQN hits a thunderstorm area, which consequently leads to spallation and formation of the BL according to the proposal (17). Assuming that every AQN which hits the area under thunderclouds (where ionization is high and spallation is likely to occur) produces a single secondary AQN_s , we arrive to the following estimate for the BL flux within AQN framework:

$$\frac{d\Phi_{\text{BL}}^{\text{AQN}}}{dA} \approx \frac{d\Phi}{dA} \cdot \mathcal{F} \approx 4 \cdot 10^{-2} \mathcal{F} \left(\frac{\rho_{\text{DM}}}{0.3 \text{ GeV cm}^{-3}} \right) \frac{(\text{BL events})}{\text{yr} \cdot \text{km}^2}, \quad (34)$$

where parameter \mathcal{F} describes the fraction of time when the area dA has been under thunderclouds.

We present two different estimates for parameter \mathcal{F} below. First estimation of parameter \mathcal{F} is based on compilation of the annual thunderstorm duration from 450 air weather system in USA as described in [43].

⁷In fact, there are many models suggesting that BL is formed as a result of lightnings.

The corresponding estimates suggest that on average the thunderstorms last about 1% of time in each given area [43]. If we adopt this estimate we arrive to conclusion that

$$\frac{d\Phi_{\text{BL}}^{\text{AQN}}}{dA} \approx 4 \cdot 10^{-4} \left(\frac{\rho_{\text{DM}}}{0.3 \text{ GeV cm}^{-3}} \right) \frac{(\text{BL events})}{\text{yr} \cdot \text{km}^2}, \quad \mathcal{F} \approx 10^{-2} \quad (35)$$

The second (independent) estimation of parameter \mathcal{F} has been used in our analysis [37] of mysterious CR-like events, the so-called Telescope Array bursts. This estimate is based on the number of detected lightning events during 5 years (between May 2008 and April 2013) in the area. The corresponding number of lightning events is 10073 [44, 45]. Assuming that a typical thunderstorm lasts one hour and produces 10^2 lightnings [46] one can infer that the total time when the relevant area was under a thunderstorm is $10073 \cdot 10^{-2} h \simeq 10^2 h$ during 5 years of recording. This represents approximately fraction $\mathcal{F} \simeq 0.25 \cdot 10^{-2}$. As a result we arrive to our second estimate for frequency of the BL events:

$$\frac{d\Phi_{\text{BL}}^{\text{AQN}}}{dA} \approx 10^{-4} \left(\frac{\rho_{\text{DM}}}{0.3 \text{ GeV cm}^{-3}} \right) \frac{(\text{BL events})}{\text{yr} \cdot \text{km}^2}, \quad \mathcal{F} \approx 0.25 \cdot 10^{-2}. \quad (36)$$

If efficiency of spallation which produces the secondary AQN_s from original AQN is less than 100% the corresponding estimates (35) and (36) decrease correspondingly. If original AQN produces (as a result of spallation) more than one AQN_s than the corresponding estimates (35) and (36) increase correspondingly.

With all these theoretical uncertainties mentioned above, we consider our estimates (35) and (36) are perfectly consistent with lower bound (32). In fact, it is amazing that so different estimates which include dramatically different environments and physical systems (from thunderstorms and lightning events to dark matter density ρ_{DM} and galactic wind velocities explicitly entering all the estimates) are so close to each other.

Precisely the estimates (35) and (36) answer (within the AQN framework) the question formulated in the first paragraph of this section: why the BL events are so rare? The proposed answer is that the rareness of BL events is a consequence of the rareness of the AQN events with very tiny DM flux (33).

We conclude this section with the following comment. The consistency of our estimates (35) and (36) with lower bound (32) along with multiple consistency checks summarized in Sect.3.8 further strengthen the proposal (17) relating BL and DM physics.

5. On Possible relation between BL and other Unidentified Aerial Phenomena (UAP)

In this section we would like to present several arguments suggesting that some of the Unidentified Aerial Phenomena (UAP) might be also related to the DM physics. For a comprehensive review on UAP observations see recent review [47].

By obvious reasons this section is much more speculative in comparison with all our previous sections because of scarcely real physical measurements of UAP events in comparison with sufficiently long list of numerical estimates for BL events as reviewed in Sect. 1.1. In fact, items (ix), (x) and (xi) from Sect. 1.1 can be treated as the BL-features recorded by modern physics instruments. This should be contrasted with UAP-related phenomena when very few observations could be considered as well documented and properly recorded events. In fact, scientific studies of the UAP phenomena started very recently, see e.g. papers [48–50]. Nevertheless, we opted to include descriptions of several such observations into this work because we believe that some of the UAP observations might be closely related to BL physics. Therefore, some UAP events may also represent the manifestations of the DM physics as a consequence of our proposal (17).

Indeed, there is one unique but crucial common element relating BL phenomena and UAP: in both cases no any material objects remain in the active area where events took places. This is in spite of the fact that many secondary accompanying effects had been observed and even measured in physics laboratories. The secondary effects manifested in many different ways: in form of the visible light, X rays, shock acoustic waves (see Sect. 5.2), heat melting the glass or soil (see Sect.5.1). This is only possible when the source of the energy for both cases is represented by annihilation processes of the antimatter with surrounding matter materials, which is precisely the key element of this proposal.

As a result of these similarities we propose that some of the UAP events may be also considered as profound manifestations of the same DM physics similar to our proposal (17) relating BL and DM physics. Therefore, the main purpose of this section is to argue that many UAP events are in fact very similar to the BL phenomena discussed in Sect. 3. The only difference is that the UAP events are characterized by dramatically different energy scales (larger baryon charge, and consequently much higher velocity at the moment of observation) in comparison with BL events with low velocities and typical energies (18).

5.1. Pseudo-meteorites events as the AQN-induced events

There are many reports in the literature describing the meteor-like events which (after detail studies by professionals) turned out to be not the meteorites. The corresponding events are classified as “Pseudo-meteorites events”, see [51] with large number of references and details. In this work we want to focus on a single event which took place in US town of Elma (Washington State) on July 15, 2003 as described in [51]. Many other similar events discussed in [51] shall not be mentioned here, and we think they likely have the same nature, and are originated from the same physics.

The key elements of the Elma event are [51]: 1. after the event (fireball) the glassy black rocks had been found; 2. the rocks were very hot (one of the witnesses had burned a thumb and a finger by collecting the rocks); 3. analysis of the discovered stones by the University of Washington concluded that the glassy rocks were not meteorites, see pictures in [51]; 4. security cameras did not record any suspicious images; 5. cloud of dust went up in the active area.

Our original comment is as follows. The Elma event is very similar to BL events discussed in Sect. 3 with the only difference is that the AQN_s must be much larger in size $B \gg 10^{15}$ in comparison with a typical BL event. In this case, as we discussed in item 3 in Sect. 3.6 the AQN_s cannot efficiently slowdown, and it is likely to hit the earth’s surface with a high speed. As a result, the AQN_s gets annihilated in deep underground regions (not in air, which is typical for BL events) by heating the surrounding rocks along its path. In many respects the heating of the surrounding material is similar to phenomena of the BL passing through the glass window when the internal AQN_s temperatures could reach enormous values due to much higher density of the soil in comparison with air, see our estimates in Sect. 3.5. It explains the hot glassy rocks found in the area. Furthermore, for the AQN_s moving with a high speed the radiation in visible frequency bands is suppressed (similar to ELFO event discussed in next Sect. 5.2), in contrast with slow moving BL discussed in Sect. 3.3. It explains the absence of any images by security camera. This identification of the “Pseudo-meteorites events” with AQN_s events is consistent with all observed puzzling observations listed in previous paragraph. Therefore, we speculate that the “Pseudo-meteorites events” along with BL events represent the right hand side of the same identification (17) and both types of events represent profound manifestations of the same DM physics.

5.2. Sky-quakes as the AQN events

The so-called skyquakes have been known for centuries, similar to BL events. They manifested in the form of sound and infrasound without leaving any physical material objects in the area in form of true meteorities. Their nature remains unknown in spite of the long history of observations, with records going back over 200 years. It has been speculated in [31] that skyquakes could be a manifestation of the dark matter AQN traveling in the atmosphere.

Unfortunately, it is next to impossible to extract any useful quantitative information from the numerous but random and unsystematic records on sky-quakes collected for centuries (very similar to BL events). Luckily, one such event which occurred on July 31-st 2008 was properly recorded by the dedicated Elginfield Infrasound Array (ELFO) near London, Ontario, Canada, see [31] for references and details. The infrasound detection was accompanied by non-observation of any meteors by an all-sky camera network, ruling out a conventional meteor source. In addition, no any meteorites had been found in the active area, similar to Elma event mentioned above in Sect. 5.1 and classified as “Pseudo-meteorites events”. Anthropogenic sources such as operations at the nearby Bruce Nuclear Power Plant or the Goderich salt mine were also eliminated; a local airport radar reported no aircraft in the area at the time. In addition to infrasound, impulses were also observed seismically (few moments after the event) as ground-coupled acoustic waves

around Southwestern Ontario and Northern Michigan. This event was treated as AQN-induced event as discussed in detail in [31] where it was argued that the energetics, infrasound-frequency properties, and other characteristics of the event are consistent with observed ELFO event.

Our original comment here is as follows. As argued in [31] the skyquakes could be also AQN induced events. However, the scale of skyquakes are dramatically different from BL events and “Pseudo-meteorites events” mentioned above. In fact, it was estimated in [31] that the the baryon charge of ELFO event is around $B \approx 10^{27}$ which is two orders of magnitude above a typical AQN size⁸ and many orders of magnitude above a typical AQN_s scale. In different words, skyquakes are the manifestations of the original AQN, not secondary AQN_s with dramatically smaller sizes and masses (and consequently released energies). However, all types of events discussed above (BL, Pseudo-meteorites, and skyquakes) can be considered as different manifestations of the same AQN-induced events when the source of the energy is the same, and it is hidden in form of the antimatter nuggets which had been produced during the QCD epoch in early Universe.

5.3. Unidentified Anomalous Vehicles (UAV) as manifestation of the AQN events

This is the most speculative subsection of this work as no quantitative physical measurements exist of the so-called Unidentified Anomalous Vehicles (UAV) which have been observed globally, see recent review [47] and scientific publication [52] with specific numerical estimates for the velocity and acceleration of UAV which seem to be inconsistent with laws of physics if interpreted as aircraft.

We interpret the radar information of the UAV image from USS Nimitz nuclear aircraft carrier (14 November 2004), see Fig. 5 in [52], as an image of a highly ionized cloud (cylindrical form) produced by passing AQN. In what follows we support this interpretation by estimation of the plasma frequency ω_p of this ionized cloud. In this case the pulse being sent from radar will be reflected by this highly ionized cloud and recorded by USS Nimitz. The effect of reflection from ionized cloud is similar to reflection of the AM radio bands from the Earth’s ionosphere. In contrast with ionosphere however where $\omega_p \approx 2 \cdot 10^7 s^{-1}$ (MHz range), the plasma frequency in highly ionized cloud produced by passing AQN could easily assume GHz range. As a result, the AQN-induced cloud could be misinterpreted as UAV image. In what follows we support our proposal by providing an order of magnitude estimates for ω_p and the size of the highly ionized cloud produced by passing AQN.

Indeed, our order of magnitude estimates as given in Appendix C suggest that the AQN propagating at high altitudes will be ionizing the surrounding area with very high efficiency. We estimated the plasma frequency for this ionized region to be on the level $\omega_p \approx 3 \cdot 10^9 s^{-1}$ or even much higher, according to (52). This implies that the pulses with GHz frequency bands from radar can be reflected by the ionized cloud⁹, which can be misinterpreted as UAV. Furthermore, a typical size of the cloud is determined by the mean free path of the 20 keV photons emitted by very hot AQN. The corresponding mean free path is estimated in (50) and it assumes the numerical value around $L_\gamma \approx 15$ m. This scale is similar to the size of UAV image mentioned in ref. [52]. Finally, the acceleration and the velocity of the AQN propagating in atmosphere have been estimated in (44) and (47) and consistent with the values presented in ref. [52]. The estimation (47) shows that the acceleration could easily reach enormous magnitudes $\sim (10^2 - 10^4)g$ being inconsistent with modern technology if interpreted as UAV according to ref. [52]. Of course, such acceleration is perfectly consistent with physics laws if interpreted as the AQN object which enters the earth’s atmosphere with galactic velocity (around $10^{-3}c$) and slows down as a result of collisions with atoms and molecules in atmosphere as described in Appendix B.

We conclude this section by mentioning that UAV along with BL, Pseudo-meteorites, and skyquakes as discussed above represent different manifestations of the same AQN-induced events when the source of the energy is hidden in the antimatter nuggets which had been formed during the QCD epoch in early Universe.

⁸Such powerful events are much more rare ones than typical AQN events with rate given by (8) because the size distribution $f(B) \propto B^{-2}$

⁹One should emphasize that an ionized cloud produced by passing AQN is the subject of atmospheric currents and can easily move and fluctuate. The AQN itself entering the atmosphere with very high speed $\sim 10^{-3}c$ could be at a very different location at the instant when the radar records the image of the ionized cloud.

All these events are very rare ones. Their rareness is explained by very tiny DM flux formulated in terms of the well-constrained DM density ρ_{DM} as given by (33).

It is obvious that we can not make any progress in understanding of the UAP events mentioned above due to the lack of real data and proper physics measurements, which makes this section even more speculative than BL studies with sufficiently long list of numerical estimates as reviewed in Sect. 1.1. Fortunately, the situation is about to change, and a number of projects and proposals, see e.g. [48–50] have been put forward to fill this gap. The UAP events in general and UAV events in particular can be and should be systematically studied. We propose in Sect. 6.2 several specific tests on how to substantiate or refute our proposal formulated above on identification some of the UAP events with AQN-induced phenomena.

6. Concluding comments and Future Developments

The presence of the *antimatter* nuggets¹⁰ in the system implies, as reviewed in Sect.2, that there will be annihilation events leading to enormous energy injection into surrounding region. As a result of these annihilation events one should anticipate a large number of observable effects on different scales: from Early Universe to the galactic scales to the Sun and the terrestrial events.

In the present work we focused on manifestations of these annihilation events on possible resolution of the mysterious BL physics. In next Section 6.1 we suggest specific tests which could support or refute the proposed resolution of these BL-related mysteries. In Section 6.2 we suggest different types of experiments with the instruments which could support or refute our suggestion that some UAP events (such as Pseudo-meteorites, skyquakes, UAV) could be also related to the AQN-induced phenomena as argued in Sect.5. Finally, in Sect. 6.3 we overview other manifestations of the same AQN framework at dramatically different scales: from the early Universe to galactic scales, to the solar scale to the Earth scale, where similar mysterious puzzles are known for decades (even centuries), and could be also related to the same antimatter nuggets (representing the DM objects) within the same AQN framework. We emphasize that the parameters of the model were fixed long ago irrespective to the BL or UAP physics which represents the topic of the present work.

6.1. BL as manifestation of the AQN_s events. Possible future tests of the proposal (17).

We already formulated the basic results demonstrating the consistency of the proposal (17) with observed BL features in Sect. 3.8. We do not need to repeat these results again. Instead, we focus here on possible future tests of the proposal (17). Before we formulate the basic idea for the test we would like to make few comments on observed anomalous and mysterious cosmic rays (CR)-like events which are very hard to explain within conventional framework and modelling. These events are strongly associated with thunderstorm and lightning events in the area, similar to BL events discussed in this work.

In particular, the Telescope Array (TA) collaboration [44, 45] reported the observations of mysterious bursts when at least three air showers were recorded within 1 ms which cannot occur with conventional high energy CR (it should be days or event months for two or more consecutive energetic CR events hit the same area). These TA mysterious bursts are associated with lightning events in the area. We proposed in [37] that these puzzling events could be related to the AQN-induced events. In fact, in ref. [37] we used the same formula (33) for estimation of the rate of TA mysterious bursts which was used for estimation of the BL frequency of appearance in (36). We explained the rareness of these TA mysterious bursts precisely in the same way as the rareness of BL events.

Similar “Exotic Events” recorded by the AUGER collaboration [53–55] are also associated with thunderstorm activity in the area. These events also cannot be explained by canonical CR modelling. At the same time, these “Exotic Events” recorded by the AUGER collaboration can be explained within AQN

¹⁰We remind the readers that the antimatter in this framework was suggested long ago [6, 7] as natural resolution of two fundamental cosmological puzzles: 1. similarity between visible and DM components, $\Omega_{\text{DM}} \sim \Omega_{\text{visible}}$; 2. observed baryon asymmetry of our Universe. These puzzles are automatically resolved in the AQN framework irrespective to the parameters of the model. A mechanism of formation of these antimatter nuggets is reviewed in Sect. 2.

framework as argued in [35]. Furthermore, the rareness of these “Exotic Events” is also explained in the AQN framework by same formula (33) and it is consistent with counting of the “Exotic Events” by the AUGER collaboration.

We mentioned these two studies on unusual CR like events to propose to test the hypothesis (17) as follows. If one can install all sky cameras, similar to the ones used in analysis [11], to monitor entire sky in the same area where TA or AUGER detectors (or any other CR labs) are located one can record the BL events with frequency of appearance similar to mysterious bursts recorded by TA collaboration or “Exotic Events” recorded by AUGER collaboration¹¹. Indeed, in all cases the basic formula describing the rate for all these events is (36). This formula is shown to be consistent with TA mysterious bursts (10 events recorded during 5 years), AUGER “Exotic Events” (23 events recorded during 13 years). The same formula is also consistent with lower bound for BL events (32) as discussed in Sect. 4. Therefore, we predict (within AQN framework) that the rate for BL events in the area will be similar to observed TA mysterious bursts events and AUGER “Exotic Events” because all these events are different manifestations of the same DM physics.

Furthermore, we also predict, within the same AQN framework, that TA mysterious bursts will be correlated in time with observations of the BL in the same area under thunderstorm. The same comment obviously applies to AUGER “Exotic Events”. The recording of such correlation would be very strong and unambiguous argument supporting entire idea about the nature of BL as profound manifestation of the DM physics, as advocated in this work.

6.2. UAP as manifestation of the AQN events. Possible future tests.

In this subsection we would like to make few comments on possible tests of our interpretation of some UAP events as discussed in Section 5 as the direct manifestation of the AQN events, similar to our interpretation of the BL events as the AQN_s events. However, in contrast with proposed tests in previous subsection 6.1 the required instruments to detect the signals from UAP should be very different as they must be sensitive to very different frequency bands.

Therefore, based on the discussions in Sections 5.2 and 5.3 we suggest to test our proposal relating BL, Pseudo-meteorites, skyquakes and UAV phenomena with AQN-induced effects (representing the DM physics in this framework) as follows. First of all, one can search for infrasound acoustic signals, similar to our suggestion formulated in [31] where we proposed to use Distributed Acoustic Sensing (DAS), which is becoming a conventional tool for seismic and other applications. The basic idea of these activities can be explained as follows. It has been known for quite sometime that distributed optical fiber sensors are capable of measuring the signals at thousands of points simultaneously using an unmodified optical fiber as the sensing element. The recent development is that the DAS is capable of measuring strain changes at all points along the optical fiber at *acoustic frequencies*, which is crucial for our studies of the acoustic waves emitted due to the AQN passage.

Another element which could play a crucial role in identification of the UAV is the radar. We suggest to use two different frequencies simultaneously, one is with larger than plasma frequency, $\omega > \omega_p$ and another one is with smaller than plasma frequency $\omega < \omega_p$. The radar with $\omega < \omega_p$ will detect the image of the ionized cloud produced by the passing AQN, while another radar with $\omega > \omega_p$ will be blind to the same area. The recording of the correlation between two radars with different frequencies and DAS should be considered as a very strong and unambiguous argument supporting entire idea about the nature of UAP as profound manifestation of the DM physics in form of the antimatter nuggets powering all these mysterious events. The event rate is determined by the DM flux (33) which is consistent with the BL lower bound as discussed in Section 4, and consistent with observed mysterious and anomalous events (which we believe are consequences of the AQN events) recorded by AUGER and Telescope Array collaborations as reviewed in Section 6.1.

¹¹Similar all sky camera had been used by monitoring entire sky in connection with studies of the meteoroids, and searches for correlations with infrasound signals, see Section 5.2.

6.3. Other (indirect) evidences for DM in form of the AQN

There are many hints suggesting that the annihilation events and consequent energy injection into space (which is inevitable feature of this framework) may indeed took place in early Universe, during the galaxy formation as well as in present epoch. We would like to mention (for completeness of the presentation) a number of mysterious puzzles at different scales which could be also related to the additional energy injection induced by the AQN annihilations events with surrounding material.

We start this list of (yet) unresolved puzzles from early Universe epoch, more specifically with BBN when the so-called the “Primordial Lithium Puzzle” has been with us for decades. It has been argued in [27] that the AQNs during the BBN epoch do not affect BBN production for H and He, but might be responsible for a resolution of the “Primordial Lithium Puzzle” due to the Li large electric charge $Z = 3$ strongly interacting with negatively charged AQN.

Another well known puzzle is related to the galaxy formation epoch. The corresponding puzzles commonly are formulated as “Core-Cusp Problem”, “Missing Satellite Problem”, “Too-Big-to-Fail Problem”, to name just a few, see recent reviews [15, 56] for the details¹². It has been argued in [57] that the aforementioned discrepancies (and many other related problems referred to in footnote 12) may be alleviated if dark matter is represented in form of the composite, nuclear density objects within AQN framework.

We now move from the early times in evolution of the Universe to the present day observations. In this case there is a set of puzzles which is related to the diffuse UV emission in our galaxy. It has been claimed in [58–60] that there are many observations which are very hard to understand if interpreted in terms of the conventional astrophysical phenomena. The analysis [58–60] very convincingly disproves the conventional picture that the dominant source of the diffused UV background is the dust-scattered radiation of the UV emitting stars. The arguments are based on a number of very puzzling observations which are not compatible with standard picture. First, the diffuse radiation is very uniform in both hemispheres, in contrast to the strong non-uniformity in distribution of the UV emitting stars. Secondly, the diffuse radiation is almost entirely independent of Galactic longitude. This feature must be contrasted with localization of the brightest UV emitting stars which are overwhelmingly confined to the longitude range $180^{\circ} - 360^{\circ}$. These and several similar observations strongly suggest that the diffuse background radiation can hardly originate in dust-scattered starlight. The authors of [58] conclude that the source of the diffuse FUV emission is unknown –that is the mystery that is referred to in the title of the paper [58].

It has been proposed in [61] that this excess in UV radiation could be a result of the dark matter annihilation events within the AQN dark matter model. The proposal [61] is supported by demonstrating that intensity and the spectral features of the AQN induced emissions are consistent with the corresponding characteristics of the observed excess [58–60] of the UV radiation.

We move from galactic to solar scale. The AQNs might be also responsible for renowned long standing problem¹³ of the “Solar Corona Mystery” when the so-called “nanoflares” conjectured by Parker long ago [64] are identified with the annihilation events in the AQN framework[62, 63].

We move from solar scale to terrestrial unusual events. We already mentioned mysterious CR like events in Sect. 6.1. There are many other terrestrial unusual events when conventional picture cannot explain the observed phenomena. In particular, the ANITA observed two anomalous events with non-inverted polarity [65, 66]. Such events correspond to very large inclination angle when “something” crossing the earth before exiting from opposite side of earth at the moment of recording by ANITA. Such events are very hard to explain within conventional physics, but could be explained within AQN framework [67].

¹²There are many more similar problems and very puzzling observations. We refer to the review papers [15, 56] on this matter. There are also different, but related observations which apparently inconsistent with conventional picture of the structure formation [56].

¹³This persisting puzzle is characterized by the following observed anomalous behaviour of the Sun: the quiet Sun (magnetic field $B \sim 1$ Gauss) emits an extreme ultra violet (EUV) radiation with a photon energy of order 10^2 eV which cannot be explained in terms of any conventional astrophysical phenomena. This happens within an atmospheric layer thickness of only 100 km or even much less. The variation of EUV with solar cycles is very modest and of order of (20-30)% during the solar cycles when magnetic activity varies by factor 10^2 or more. So, it is hard to imagine how the magnetic reconnection, which is known to be responsible for large flares, could play any role when $B \sim 1$ Gauss. There are many other puzzling features discussed in [62, 63].

Finally, it has been recently argued in [68, 69] that numerous enigmatic observations remain challenging to explain within the framework of conventional physics. In particular, these anomalies include unexpected correlations between temperature variations in the stratosphere and the total electron content of the Earth's atmosphere (along with many other mysterious correlations), such that entire globe can be thought as a one large detector. Decades of collected data provide statistically significant evidence for these observed correlations. However, no any conventional explanations for such mysterious correlations had been offered. It has been argued in [70] that the recorded correlations can be generated by the AQN-induced processes.

We conclude this work with the following final comment. We advocate an idea that the BL known for centuries might be a profound manifestation of the DM physics when DM is made of (anti)quarks and gluons of the Standard Model as reviewed in Sect.2. We also speculate that other mysterious phenomena known as UAP (it includes pseudo-meteorites, skyquakes and UAV) might also represent different manifestations of the same AQN dark matter physics. The AQN dark matter model is consistent with all presently available cosmological, astrophysical, satellite and ground-based observations. In fact, it may even shed some light on the long standing puzzles and mysteries as briefly reviewed above in Section 6.3. If validated through the proposed tests and experiments, this framework could revolutionize our understanding of DM and its role in the cosmos. The BL and UAP events as profound direct manifestations of the DM on earth (within the AQN framework) could play a key role in the *direct* study of the DM in scientific labs, in contrast with *indirect* manifestations of the AQN-induced phenomena reviewed in Sect. 6.3.

Acknowledgements

This research was supported in part by the Natural Sciences and Engineering Research Council of Canada.

A. AQN emission spectrum

The goal of this Appendix is to overview the spectral characteristics of the AQNs as a result of annihilation events when the nugget enters the Earth atmosphere. The corresponding computations have been carried out in [36] in application to the galactic environment with a typical density of surrounding visible baryons of order $n_{\text{galaxy}} \sim 1 \text{ cm}^{-3}$ in the galaxy. We review these computations with few additional elements which must be implemented for Earth's atmosphere when typical density of surrounding baryons is much higher $n_{\text{air}} \sim 10^{21} \text{ cm}^{-3}$.

The spectrum of nuggets at low temperatures was analyzed in [36] and was found to be,

$$\frac{dF}{d\omega}(\omega) = \frac{dE}{dt dA d\omega} \simeq \frac{1}{2} \int_0^\infty dz \frac{dQ}{d\omega}(\omega, z) \sim \sim \frac{4}{45} \frac{T^3 \alpha^{5/2}}{\pi} \sqrt[4]{\frac{T}{m}} \left(1 + \frac{\omega}{T}\right) e^{-\omega/T} h\left(\frac{\omega}{T}\right), \quad (37)$$

where $\alpha = 137^{-1}$ is the fine structure constant and we use units $\hbar = c = k_B = 1$. The function $Q(\omega, z) \sim n^2(z, T)$ describes the emissivity per unit volume from the electrosphere characterized by the density $n(z, T)$, where z measures the distance from the quark core of the nugget. The $\frac{dF}{d\omega}(\omega)$ describes the intensity of emission from unit area A at frequency ω at temperature T . In Eq. (37) a complicated function $h(x)$ can be well approximated as

$$h(x) = \begin{cases} 17 - 12 \ln(x/2) & x < 1, \\ 17 + 12 \ln(2) & x \geq 1. \end{cases} \quad (38)$$

Integrating over ω contributes a factor of $T \int dx (1+x) \exp(-x) h(x) \approx 60T$, giving the total surface emissivity:

$$F_{\text{tot}} = \frac{dE}{dt dA} = \int_0^\infty d\omega \frac{dF}{d\omega}(\omega) \sim \frac{16}{3} \frac{T^4 \alpha^{5/2}}{\pi} \sqrt[4]{\frac{T}{m}}. \quad (39)$$

A typical internal temperature of the nuggets can be estimated from the condition the radiative output of equation (39) must be balanced the flux of energy onto the nugget due to the annihilation events. In this case one arrives to equation (11) from the main body of the text.

The factor κ is introduced to account for complicated physics as mentioned in the main body of the text. In a neutral environment when no long range interactions exist the value of κ cannot exceed $\kappa \sim 1$ which would correspond to the total annihilation of all impacting matter into thermal photons. The high probability of reflection at the sharp quark matter surface lowers the value of κ . The propagation of an ionized (negatively charged) nugget in a highly ionized plasma will increase the effective cross section, and therefore value of κ as discussed in [63] in application to the solar corona heating problem.

For the neutral environment (such as Earth's atmosphere) and relatively low temperature when the most positrons from electrosphere remain in the system the parameter κ should assume values close to unity, i.e. $0.1 \leq \kappa \leq 1$. In this case, from (11) assuming that $0.1 \leq \kappa \leq 1$ one arrives to the estimate (13) from the main body of the text.

There are few additional elements which should be taken into account for Earth's atmosphere in comparison with original computations [36, 38] applied to very dilute galactic environment with much lower temperatures $T \simeq 1$ eV. However, these effects in general do not modify the basic scale used in the main body of the text (13).

For our analysis in Sect. 3 we need to estimate the internal temperature of the AQN_s after its complete stop when the rate annihilation is determined by typical velocities of molecules in air (25) rather by v_{AQN} itself. Due to dramatic decrease of the annihilation rate the equilibration internal temperature also decreases in comparison with (13), and can be estimated as follows:

$$T \sim 20 \text{ keV} \cdot \left(\frac{n_{\text{air}}}{10^{21} \text{ cm}^{-3}} \right)^{\frac{4}{17}} \cdot \left(\frac{v_{\text{air}}}{v_{AQN}} \right)^{\frac{4}{17}} \cdot 4^{\frac{4}{17}} \approx 6 \text{ keV}, \quad (40)$$

where factor $4^{\frac{4}{17}}$ accounts for the difference between geometrical cross section πR^2 for fast moving AQN and $4\pi R^2$ for AQN_s at rest when air molecules from all angles can hit the AQN_s . Precisely this internal temperature is our benchmark value to be used in the main body of the text.

For our analysis in Sect. 3 we also need the estimate for the effective size R_{eff} of the AQN_s after spallation. We define the effective radius R_{eff} as the scale where positrons from electrosphere remain to be strongly bound to the quark's core at the internal temperature $T \approx 6$ keV. The corresponding scale can be estimated from the condition that the binding energy of the positrons is approximately equal to internal temperature T of the system, similar to our previous estimates for the galactic environment [36, 38], i.e.

$$\frac{\alpha Q_{AQN_s}}{R_{\text{eff}}} \approx T \approx 6 \text{ keV} \quad \rightarrow \quad R_{\text{eff}} \approx 10^{-6} \text{ cm}, \quad [\text{to be identified with internal size of an } AQN_s] \quad (41)$$

where we use estimate (19) for Q_{AQN_s} . As expected R_{eff} is dramatically larger than $R \approx 10^{-8}$ cm from (18) corresponding to the size of the quark matter core itself. One should emphasize that the physical meaning of the scale R_{eff} is very different from the scales discussed in Sects. 3.3 and 3.5. The R_{eff} literally describes the internal structure of the AQN_s as the positrons from electrosphere are strongly bound to the quark core. It must be contrasted with the scales from Sects. 3.3 and 3.5 which describe the mean free paths of the photons emitted from electrosphere. These structures (including visible size of BL) emerge as a result of the interaction with surrounding material. In other words, these scales are determined by the environment where AQN_s propagates, rather than by internal structure of AQN_s itself.

B. The BL's stoppage time from the instant of formation to the moment of observation

The main goal of this Appendix is to provide a quantitative description of the kinematical motion of the AQN_s from the instant of formation in thunderclouds at high altitudes to the moment when it starts to behave as a typical BL object emitting the visible frequency light close to the Earth's surface. We also justify our estimate as given in Sect. 3.6 on typical time scale when BL becomes observable in visible frequency bands.

The process of slowing down of a heavy AQN entering the atmosphere has been discussed previously in the context of the solar corona in [63]. However, it can be directly applied to the AQN_s propagating in the

Earth's atmosphere which is the topic of the present work. Therefore, we can generalize formula from [63] to describe the anti-matter AQN_s moving with velocity $v_{AQNs}(t)$ in the atmosphere with matter density $\rho_{\text{air}} \approx m_p n_{\text{air}}$:

$$M_{AQNs} \frac{dv_{AQNs}(t)}{dt} \approx -\frac{\pi R_{\text{eff}}^2}{2} \cdot (m_p n_{\text{air}}) \cdot v_{AQNs}^2(t), \quad M_{AQNs} \approx m_p B_s. \quad (42)$$

In what follows we assume that B_s varies with time much slower than $v_{AQNs}(t)$, in which case B_s can be treated as constant initial baryon charge entering estimate (30) for L . In this case the equation (42) can be simplified as follows:

$$\frac{dv_{AQNs}(t)}{dt} \approx -\frac{1}{2L} \cdot v_{AQNs}^2(t). \quad (43)$$

With all these assumptions and approximations the solution for velocity $v_{AQNs}(t)$ as a function of time t assumes the form

$$\left(\frac{1}{v_{AQNs}(t)} - \frac{1}{v_{AQNs}(t_0)} \right) \approx \frac{(t - t_0)}{2L}, \quad \text{where } v_{AQNs}(t_0) \approx v_{AQNs}(t_0) \approx 10^{-3}c \quad (44)$$

Our estimate (44) suggests that a typical stoppage time scale τ_s when velocity $v_{AQNs}(\tau_s)$ assumes only $\sim 1\%$ of its initial value after spallation can be estimated as follows

$$\tau_s \approx \frac{2L}{v_{AQNs}(\tau_s)} \approx \frac{2L}{[0.01 \cdot v_{AQNs}(t_0)]} \approx \frac{6 \text{ km}}{10^{-5}c} \approx 2 \text{ s}, \quad (45)$$

which is precisely the value being used in the main body of the text in Sect. 3.6. The main argument to define stoppage time scale τ_s as the scale when velocity $v_{AQNs}(\tau_s)$ approximately assumes $\sim 1\%$ fraction from its original value 300 km/s (when DM object enters the atmosphere) is that the internal temperature of the nugget at this velocity is close to $T \approx 6$ keV. Precisely at this typical internal temperatures the BL starts to radiate efficiently in the visible frequency bands as discussed in Sect. 3.3.

Indeed, internal temperature T at the velocity $[0.01 \cdot v_{AQNs}]$ assumes the form

$$T \sim 20 \text{ keV} \cdot \left(\frac{n_{\text{air}}}{10^{21} \text{ cm}^{-3}} \right)^{\frac{4}{17}} \cdot \left(\frac{0.01 \cdot v_{AQNs}(t_0)}{v_{AQNs}(t_0)} \right)^{\frac{4}{17}} \approx 6.7 \text{ keV}, \quad (46)$$

and becomes very similar to the temperature (40) we used in our analysis in Sect. 3.3.

The equation (44) allows us to estimate a typical acceleration of the BL after spallation time at t_0 as follows:

$$a_{v_{AQNs}} \equiv \frac{v_{AQNs}(t)}{dt} \approx -\frac{2L}{(t - t_0)^2} \approx 1.5 \cdot 10^3 \frac{\text{m}}{\text{s}^2} \cdot \left(\frac{\tau_s}{(t - t_0)} \right)^2 \gg 10^2 g. \quad (47)$$

The estimate (47) shows that the acceleration of the AQN_s could be enormous and could easily exceed $10^2 g$ as a result of very strong friction as it propagates in atmosphere. In fact it could easily exceed $10^4 g$ at $(t - t_0) \approx 0.1\tau_s \approx 0.2s$ when the velocity of the AQN_s already dropped by 90% from its original value to reach 30 km/s. Such enormous acceleration had been mentioned previously in the literature [52] in relation with Unidentified Aerial Phenomena (UAP). We discuss a possible relation between BL and UAP phenomena in the main body of the text in Sect. 5.

C. On ionization of air along the AQN path

The main goal of this appendix is to estimate the plasma frequency ω_p which is the basic element of the discussions of Sect. 5.3. The plasma frequency ω_p characterizes the propagation of photons in the ionized plasma. The ω_p can be thought as an effective mass for photon: only photons (from radar) with the energy larger than this mass can propagate in ionized plasma, while photons with $\omega < \omega_p$ will be reflected by ionized

plasma back to the radar producing the corresponding image of the ionized cloud. The relevant formula for ω_p reads:

$$\omega_p^2 = \frac{4\pi\alpha n_{\text{ion}}}{m}. \quad (48)$$

To estimate ω_p we have to estimate the density of the ions n_{ion} which will be produced along the AQN path. The corresponding estimates had been performed in [31] and we use formula (9) from that work

$$E_l \simeq 10^4 \cdot \left(\frac{B}{10^{25}}\right)^{2/3} \left(\frac{n_{\text{air}}}{10^{21} \text{ cm}^{-3}}\right) \frac{\text{J}}{\text{m}}, \quad (49)$$

where E_l has the physical meaning of the energy per unit length injected along the AQN's path. The energy injection in [31] was estimated at the sea level. For energy injection at high altitudes z one should insert factor $\exp(-z/h)$ accounting for density decrease with altitude, see (50) below. After that one can estimate the number of emitted photons per unit length along the AQN's path by dividing E_l to the internal temperature of the nugget, i.e. E_l/T .

The next step is to estimate the photon's mean free path L_γ at high altitude $z \approx 8.5$ km where UAV had been observed. It has been also computed in [31] for the sea level altitude and we use formula (12) from that work with adjustment for the altitude dependence:

$$L_\gamma(z) = \frac{\lambda}{\rho_{\text{air}}(z)} \simeq 5\text{m} \cdot \exp\left(\frac{z}{h}\right) \approx 15\text{m}, \quad \text{where } h \approx 8 \text{ km}. \quad (50)$$

The next step is to estimate the density of the ions n_{ion} along the AQN propagation's path as follows:

$$n_{\text{ion}} \approx \frac{E_l(z)}{[\pi L_\gamma^2(z) \cdot T]} \approx 2 \cdot 10^9 \frac{\text{ions}}{\text{cm}^3}, \quad (51)$$

where we assume that every $T \approx 20$ keV photon (which is our benchmark value) produces a single ion (through the photo-effect as discussed in Sect. 3.3). We consider this estimate as a very conservative assumption as 20 keV injected energy is capable to produce multiple ions through the chain of processes, such that the n_{ion} could be in fact much higher than estimate (51) suggests.

The final step in our estimate is to substitute (51) into expression (48) for the plasma frequency to arrive

$$\omega_p = \sqrt{\frac{4\pi\alpha n_{\text{ion}}}{m}} \approx 3 \cdot 10^9 \text{ s}^{-1}, \quad (52)$$

which corresponds to the GHz range. This estimate is used in the main body of the text in Sect. 5.3.

References

- [1] H. Boerner, *Ball Lightning*, Springer Cham, 2019, pp. 1–205.
URL <https://doi.org/10.1007/978-3-030-20783-0>
- [2] B. Smirnov, *Physics of ball lightning*, *Physics Reports* 224 (4) (1993) 151–236. doi:[https://doi.org/10.1016/0370-1573\(93\)90121-S](https://doi.org/10.1016/0370-1573(93)90121-S).
URL <https://www.sciencedirect.com/science/article/pii/037015739390121S>
- [3] M. L. Shmatov, K. D. Stephan, *Advances in ball lightning research*, *Journal of Atmospheric and Solar-Terrestrial Physics* 195 (2019) 105115. doi:<https://doi.org/10.1016/j.jastp.2019.105115>.
URL <https://www.sciencedirect.com/science/article/pii/S1364682619303840>
- [4] V. A. Rakov, M. A. Uman, *Ball lightning, bead lightning, and other unusual discharges*, Cambridge University Press, 2003, p. 656?674.
URL <https://www.cambridge.org/core/books/abs/lightning/ball-lightning-bead-lightning-and-other-unusual-discharges/13E6CD33A72BCD71D7FCE78894FB3934>
- [5] A. G. Keul, *A brief history of ball lightning observations by scientists and trained professionals*, *History of Geo- and Space Sciences* 12 (1) (2021) 43–56. doi:[10.5194/hgss-12-43-2021](https://doi.org/10.5194/hgss-12-43-2021).
URL <https://hgss.copernicus.org/articles/12/43/2021/>
- [6] A. R. Zhitnitsky, ‘Nonbaryonic’ dark matter as baryonic colour superconductor, *JCAP*10 (2003) 010. arXiv:[hep-ph/0202161](https://arxiv.org/abs/hep-ph/0202161), doi:[10.1088/1475-7516/2003/10/010](https://doi.org/10.1088/1475-7516/2003/10/010).

- [7] A. Zhitnitsky, Axion quark nuggets. Dark matter and matter–antimatter asymmetry: Theory, observations and future experiments, *Mod. Phys. Lett. A* 36 (18) (2021) 2130017. [arXiv:2105.08719](#), [doi:10.1142/S0217732321300172](#).
- [8] K. D. Stephan, Could Ball Lightning Be Magnetic Monopoles? (8 2024). [arXiv:2408.10289](#).
- [9] J. P. Ralston, Is Ball Lightning a Signal of Magnetic Monopoles? (10 2024). [arXiv:2411.00240](#).
- [10] V. L. Bychkov, A. I. Nikitin, I. P. Ivanenko, T. F. Nikitina, A. M. Velichko, I. A. Nosikov, [Ball lightning passage through a glass without breaking it](#), *Journal of Atmospheric and Solar-Terrestrial Physics* 150–151 (2016) 69–76. [doi:https://doi.org/10.1016/j.jastp.2016.10.018](#).
URL <https://www.sciencedirect.com/science/article/pii/S1364682616303595>
- [11] J. Cen, P. Yuan, S. Xue, [Observation of the optical and spectral characteristics of ball lightning](#), *Phys. Rev. Lett.* 112 (2014) 035001. [doi:10.1103/PhysRevLett.112.035001](#).
URL <https://link.aps.org/doi/10.1103/PhysRevLett.112.035001>
- [12] T. An, P. Yuan, J. Cen, S. Xue, R. Wan, H. Deng, G. Liu, X. Wang, [Temperature of apparent natural ball lightning obtained by examination of the spectra](#), *Physics of Plasmas* 29 (11) (2022) 113503. [arXiv:https://pubs.aip.org/aip/pop/article-pdf/doi/10.1063/5.0098329/16630169/113503_1_online.pdf](#), [doi:10.1063/5.0098329](#).
URL <https://doi.org/10.1063/5.0098329>
- [13] K. D. Stephan, R. Krajcik, R. J. Martin, [Fluorescence caused by ionizing radiation from ball lightning: Observation and quantitative analysis](#), *Journal of Atmospheric and Solar-Terrestrial Physics* 148 (2016) 32–38. [doi:https://doi.org/10.1016/j.jastp.2016.08.005](#).
URL <https://www.sciencedirect.com/science/article/pii/S1364682616301997>
- [14] K. D. Stephan, [New observation and analysis of window damage as evidence for energy and power content of ball lightning](#), *Journal of Atmospheric and Solar-Terrestrial Physics* 261 (2024) 106300. [doi:https://doi.org/10.1016/j.jastp.2024.106300](#).
URL <https://www.sciencedirect.com/science/article/pii/S1364682624001287>
- [15] S. Tulin, H.-B. Yu, [Dark Matter Self-interactions and Small Scale Structure](#), *Phys. Rept.* 730 (2018) 1–57. [arXiv:1705.02358](#), [doi:10.1016/j.physrep.2017.11.004](#).
- [16] E. Witten, [Cosmic separation of phases](#), *Phys. Rev. D* 30 (1984) 272–285. [doi:10.1103/PhysRevD.30.272](#).
- [17] E. Farhi, R. L. Jaffe, [Strange matter](#), *Phys. Rev. D* 30 (1984) 2379–2390. [doi:10.1103/PhysRevD.30.2379](#).
- [18] A. De Rújula, S. L. Glashow, [Nuclearites - A novel form of cosmic radiation](#), *Nature* 312 (1984) 734–737. [doi:10.1038/312734a0](#).
- [19] M. ALTSCHELER, L. HOUSE, [Is ball lightning a nuclear phenomenon ?](#), *Nature*. 228 (1970) 545.
URL <https://doi.org/10.1038/228545a0>
- [20] D. Ashby, C. Whitehead, [Is ball lightning caused by antimatter meteorites?](#), *Nature*. 230 (1971) 180.
URL <https://doi.org/10.1038/230180a0>
- [21] K. Lawson, X. Liang, A. Mead, M. S. R. Siddiqui, L. Van Waerbeke, A. Zhitnitsky, [Gravitationally trapped axions on Earth](#), *Phys. Rev. D* 100 (4) (2019) 043531. [arXiv:1905.00022](#), [doi:10.1103/PhysRevD.100.043531](#).
- [22] X. Liang, A. Zhitnitsky, [Axion field and the quark nugget’s formation at the QCD phase transition](#), *Phys. Rev. D* 94 (8) (2016) 083502. [arXiv:1606.00435](#), [doi:10.1103/PhysRevD.94.083502](#).
- [23] S. Ge, X. Liang, A. Zhitnitsky, [Cosmological C P -odd axion field as the coherent Berry’s phase of the Universe](#), *Phys. Rev. D* 96 (6) (2017) 063514. [arXiv:1702.04354](#), [doi:10.1103/PhysRevD.96.063514](#).
- [24] S. Ge, X. Liang, A. Zhitnitsky, [Cosmological axion and a quark nugget dark matter model](#), *Phys. Rev. D* 97 (4) (2018) 043008. [arXiv:1711.06271](#), [doi:10.1103/PhysRevD.97.043008](#).
- [25] S. Ge, K. Lawson, A. Zhitnitsky, [Axion quark nugget dark matter model: Size distribution and survival pattern](#), *Phys. Rev. D* 99 (11) (2019) 116017. [arXiv:1903.05090](#), [doi:10.1103/PhysRevD.99.116017](#).
- [26] A. Zhitnitsky, [Cold dark matter as compact composite objects](#), *Phys. Rev. D* 74 (4) (2006) 043515. [arXiv:astro-ph/0603064](#), [doi:10.1103/PhysRevD.74.043515](#).
- [27] V. V. Flambaum, A. R. Zhitnitsky, [Primordial Lithium Puzzle and the Axion Quark Nugget Dark Matter Model](#), *Phys. Rev. D* 99 (2) (2019) 023517. [arXiv:1811.01965](#), [doi:10.1103/PhysRevD.99.023517](#).
- [28] J. Singh Sidhu, R. J. Scherrer, G. Starkman, [Antimatter as Macroscopic Dark Matter](#), *Phys. Lett. B* 807 (2020) 135574. [arXiv:2006.01200](#), [doi:10.1016/j.physletb.2020.135574](#).
- [29] O. P. Santillán, A. Morano, [Neutrino emission and initial evolution of axionic quark nuggets](#), *Phys. Rev. D* 104 (8) (2021) 083530. [arXiv:2011.06747](#), [doi:10.1103/PhysRevD.104.083530](#).
- [30] K. Lawson, A. R. Zhitnitsky, [The 21 cm absorption line and the axion quark nugget dark matter model](#), *Phys. Dark Univ.* 24 (2019) 100295. [arXiv:1804.07340](#), [doi:10.1016/j.dark.2019.100295](#).
- [31] D. Budker, V. V. Flambaum, A. Zhitnitsky, [Infrasonic, acoustic and seismic waves produced by the Axion Quark Nuggets](#), *Symmetry* 14 (2022) 459. [arXiv:2003.07363](#), [doi:10.3390/sym14030459](#).
- [32] D. M. Jacobs, G. D. Starkman, B. W. Lynn, [Macro Dark Matter](#), *Mon. Not. Roy. Astron. Soc.* 450 (4) (2015) 3418–3430. [arXiv:1410.2236](#), [doi:10.1093/mnras/stv774](#).
- [33] M. G. Alford, A. Schmitt, K. Rajagopal, T. Schäfer, [Color superconductivity in dense quark matter](#), *Rev. Mod. Phys.* 80 (2008) 1455–1515. [arXiv:0709.4635](#), [doi:10.1103/RevModPhys.80.1455](#).
- [34] S. Ge, M. S. R. Siddiqui, L. Van Waerbeke, A. Zhitnitsky, [Radio impulsive events in quiet solar corona and Axion Quark Nugget Dark Matter](#), *Phys. Rev. D* 102 (2020) 123021. [arXiv:2009.00004](#), [doi:10.1103/PhysRevD.102.123021](#).
- [35] A. Zhitnitsky, [The Pierre Auger exotic events and axion quark nuggets](#), *J. Phys. G* 49 (10) (2022) 105201. [arXiv:2203.08160](#), [doi:10.1088/1361-6471/ac8569](#).
- [36] M. M. Forbes, A. R. Zhitnitsky, [WMAP haze: Directly observing dark matter?](#), *Phys. Rev. D* 78 (8) (2008) 083505. [arXiv:0802.3830](#), [doi:10.1103/PhysRevD.78.083505](#).

- [37] A. Zhitnitsky, The Mysterious Bursts observed by Telescope Array and Axion Quark Nuggets, *J. Phys. G* 48 (6) (2021) 065201. [arXiv:2008.04325](https://arxiv.org/abs/2008.04325), [doi:10.1088/1361-6471/abd457](https://doi.org/10.1088/1361-6471/abd457).
- [38] M. M. Forbes, K. Lawson, A. R. Zhitnitsky, Electrosphere of macroscopic “quark nuclei”: A source for diffuse MeV emissions from dark matter, *Phys. Rev. D* 82 (8) (2010) 083510. [arXiv:0910.4541](https://arxiv.org/abs/0910.4541), [doi:10.1103/PhysRevD.82.083510](https://doi.org/10.1103/PhysRevD.82.083510).
- [39] M. Tanabashi, [Review of particle physics](#), *Phys. Rev. D* 98 (2018) 030001. [doi:10.1103/PhysRevD.98.030001](https://doi.org/10.1103/PhysRevD.98.030001).
URL <https://link.aps.org/doi/10.1103/PhysRevD.98.030001>
- [40] V. Berestetskii, E. Lifshitz, L. Pitaevskii, [Quantum Electrodynamics: Volume 4](#), Course of theoretical physics, Elsevier Science, 1982.
URL <https://books.google.ca/books?id=URL5NKX8vbAC>
- [41] A. V. Gurevich, K. P. Zybin, [Runaway breakdown and electric discharges in thunderstorms](#), *Physics-Uspekhi* 44 (11) (2001) 1119–1140. [doi:10.1070/pu2001v044n11abeh000939](https://doi.org/10.1070/pu2001v044n11abeh000939).
URL <https://doi.org/10.1070/pu2001v044n11abeh000939>
- [42] K. D. Stephan, R. Sonnenfeld, A. G. Keul, [First comparisons of ball-lightning report website data with lightning-location-network data](#), *Journal of Atmospheric and Solar-Terrestrial Physics* 240 (2022) 105953. [doi:https://doi.org/10.1016/j.jastp.2022.105953](https://doi.org/10.1016/j.jastp.2022.105953).
URL <https://www.sciencedirect.com/science/article/pii/S1364682622001262>
- [43] A. Gurevich, K. Zybin, High energy cosmic ray particles and the most powerful new type discharges in thunderstorm atmosphere, *Phys. Lett. A* 329 (2004) 341–347. [arXiv:hep-ex/0403050](https://arxiv.org/abs/hep-ex/0403050), [doi:10.1016/j.physleta.2004.06.094](https://doi.org/10.1016/j.physleta.2004.06.094).
- [44] R. Abbasi, et al., The bursts of high energy events observed by the telescope array surface detector, *Phys. Lett. A* 381 (32) (2017) 2565–2572. [doi:10.1016/j.physleta.2017.06.022](https://doi.org/10.1016/j.physleta.2017.06.022).
- [45] T. Okuda, [Telescope array observatory for the high energy radiation induced by lightning](#), *Journal of Physics: Conference Series* 1181 (2019) 012067. [doi:10.1088/1742-6596/1181/1/012067](https://doi.org/10.1088/1742-6596/1181/1/012067).
URL <https://doi.org/10.1088/1742-6596/1181/1/012067>
- [46] J. R. Dwyer, M. A. Uman, [The physics of lightning](#), *Phys. Rep.* 534 (4) (2014) 147 – 241, the Physics of Lightning. [doi:https://doi.org/10.1016/j.physrep.2013.09.004](https://doi.org/10.1016/j.physrep.2013.09.004).
URL <http://www.sciencedirect.com/science/article/pii/S037015731300375X>
- [47] K. H. Knuth, P. Ailleris, H. A. Agrama, E. Ansbros, T. Cai, T. Canuti, M. C. Cifone, W. B. C. Jr., F. Courtade, R. Dolan, L. Domine, L. Dini, B. Friscourt, R. Graves, R. F. Haines, R. Hoffman, H. Kayal, S. Little, G. P. Nolan, R. Powell, M. Rodeghier, E. Russo, P. Skafish, E. Strand, M. Swords, M. Szydagis, G. T. Tedesco, J. J. Tedesco, M. Teodorani, J. Vallee, M. Vaillant, B. Villarreal, W. A. Watters, [The new science of unidentified aerospace-undersea phenomena \(uap\)](#) (2025). [arXiv:2502.06794](https://arxiv.org/abs/2502.06794).
URL <https://arxiv.org/abs/2502.06794>
- [48] W. A. Watters, A. Loeb, F. Laukien, R. Cloete, A. Delacroix, S. Dobroshinsky, B. Horvath, E. Kelderman, S. Little, E. Masson, A. Mead, M. Randall, F. Schultz, M. Szenher, F. Vervelidou, A. White, A. Ahlström, C. Cleland, S. Dockal, N. Donahue, M. Elowitz, C. Ezell, A. Gersznowicz, N. Gold, M. G. Hercz, E. Keto, K. H. Knuth, A. Lux, G. J. Melnick, A. Moro-Martín, J. Martín-Torres, D. L. Ribes, P. Sail, M. Teodorani, J. J. Tedesco, G. T. Tedesco, M. Tu, M.-P. Zorzano, [The scientific investigation of unidentified aerial phenomena \(uap\) using multimodal ground-based observatories](#), *Journal of Astronomical Instrumentation* 12 (01) (2023) 2340006. [arXiv:https://doi.org/10.1142/S2251171723400068](https://arxiv.org/abs/https://doi.org/10.1142/S2251171723400068), [doi:10.1142/S2251171723400068](https://doi.org/10.1142/S2251171723400068).
URL <https://doi.org/10.1142/S2251171723400068>
- [49] L. Domine, A. Biswas, R. Cloete, A. Delacroix, A. Fedorenko, L. Jacaruso, E. Kelderman, E. Keto, S. Little, A. Loeb, E. Masson, M. Prior, F. Schultz, M. Szenher, W. A. Watters, A. White, [Commissioning an all-sky infrared camera array for detection of airborne objects](#), *Sensors* 25 (3) (2025). [doi:10.3390/s25030783](https://doi.org/10.3390/s25030783).
URL <https://www.mdpi.com/1424-8220/25/3/783>
- [50] M. Szydagis, K. H. Knuth, B. W. Kugielsky, C. Levy, Initial Results From the First Field Expedition of UAPx to Study Unidentified Anomalous Phenomena (12 2023). [arXiv:2312.00558](https://arxiv.org/abs/2312.00558).
- [51] A. Ol’khovator, Some comments on events associated with falling terrestrial rocks and iron from the sky, arXiv e-prints (2020) [arXiv:2012.00686](https://arxiv.org/abs/2012.00686), [doi:10.48550/arXiv.2012.00686](https://doi.org/10.48550/arXiv.2012.00686).
- [52] K. H. Knuth, R. M. Powell, P. A. Reali, [Estimating flight characteristics of anomalous unidentified aerial vehicles](#), *Entropy* 21 (10) (2019). [doi:10.3390/e21100939](https://doi.org/10.3390/e21100939).
URL <https://www.mdpi.com/1099-4300/21/10/939>
- [53] P. Abreu, et al., Downward Terrestrial Gamma-ray Flashes at the Pierre Auger Observatory?, *PoS ICRC2021* (2021) 395. [doi:10.22323/1.395.0395](https://doi.org/10.22323/1.395.0395).
- [54] R. Colalillo, The observation of lightning-related events with the Surface Detector of the Pierre Auger Observatory, in: *European Physical Journal Web of Conferences*, Vol. 197 of *European Physical Journal Web of Conferences*, 2019, p. 03003. [doi:10.1051/epjconf/201919703003](https://doi.org/10.1051/epjconf/201919703003).
- [55] R. Colalillo, Peculiar lightning-related events observed by the surface detector of the Pierre Auger Observatory, *PoS ICRC2017* (2017) 314. [doi:10.22323/1.301.0314](https://doi.org/10.22323/1.301.0314).
- [56] P. Salucci, N. Turini, C. Di Paolo, Paradigms and Scenarios for the Dark Matter Phenomenon, *Universe* 6 (8) (2020) 118. [arXiv:2008.04052](https://arxiv.org/abs/2008.04052), [doi:10.1142/9789811233913_0075](https://doi.org/10.1142/9789811233913_0075).
- [57] A. Zhitnitsky, Structure formation paradigm and axion quark nugget dark matter model, *Phys. Dark Univ.* 40 (2023) 101217. [arXiv:2302.00010](https://arxiv.org/abs/2302.00010), [doi:10.1016/j.dark.2023.101217](https://doi.org/10.1016/j.dark.2023.101217).
- [58] R. C. Henry, J. Murthy, J. Overduin, J. Tyler, [THE MYSTERY OF THE COSMIC DIFFUSE ULTRAVIOLET BACKGROUND RADIATION](#), *The Astrophysical Journal* 798 (1) (2014) 14. [doi:10.1088/0004-637x/798/1/14](https://doi.org/10.1088/0004-637x/798/1/14).
URL <https://doi.org/10.1088/0004-637x/798/1/14>

- [59] M. S. Akshaya, J. Murthy, S. Ravichandran, R. C. Henry, J. Overduin, [The diffuse radiation field at high galactic latitudes](#), *The Astrophysical Journal* 858 (2) (2018) 101. doi:10.3847/1538-4357/aabcb9. URL <https://doi.org/10.3847/1538-4357/aabcb9>
- [60] M. S. Akshaya, J. Murthy, S. Ravichandran, R. C. Henry, J. Overduin, Components of the diffuse ultraviolet radiation at high latitudes, *Mon. Not. R. Astron. Soc.* 489 (1) (2019) 1120–1126. arXiv:1908.02260, doi:10.1093/mnras/stz2186.
- [61] A. Zhitnitsky, The mysterious diffuse UV radiation and axion quark nugget dark matter model, *Phys. Lett. B* 828 (2022) 137015. arXiv:2110.05489, doi:10.1016/j.physletb.2022.137015.
- [62] A. Zhitnitsky, Solar Extreme UV radiation and quark nugget dark matter model, *JCAP*10 (2017) 050. arXiv:1707.03400, doi:10.1088/1475-7516/2017/10/050.
- [63] N. Raza, L. van Waerbeke, A. Zhitnitsky, Solar corona heating by axion quark nugget dark matter, *Phys. Rev. D* 98 (10) (2018) 103527. arXiv:1805.01897, doi:10.1103/PhysRevD.98.103527.
- [64] E. N. Parker, Nanoflares and the solar X-ray corona, *Astrophys. J.*330 (1988) 474–479. doi:10.1086/166485.
- [65] P. W. Gorham, et al., Characteristics of Four Upward-pointing Cosmic-ray-like Events Observed with ANITA, *Phys. Rev. Lett.* 117 (7) (2016) 071101. arXiv:1603.05218, doi:10.1103/PhysRevLett.117.071101.
- [66] P. W. Gorham, et al., Observation of an Unusual Upward-going Cosmic-ray-like Event in the Third Flight of ANITA, *Phys. Rev. Lett.* 121 (16) (2018) 161102. arXiv:1803.05088, doi:10.1103/PhysRevLett.121.161102.
- [67] X. Liang, A. Zhitnitsky, ANITA anomalous events and axion quark nuggets, *Phys. Rev. D* 106 (6) (2022) 063022. arXiv:2105.01668, doi:10.1103/PhysRevD.106.063022.
- [68] K. Zioutas, A. Argiriou, H. Fischer, S. Hofmann, M. Maroudas, A. Pappa, Y. Semertzidis, [Stratospheric temperature anomalies as imprints from the dark universe](#), *Physics of the Dark Universe* 28 (2020) 100497. doi:10.1016/j.dark.2020.100497. URL <http://dx.doi.org/10.1016/j.dark.2020.100497>
- [69] A. Argiriou, et al., Novel Dark Matter Signatures, 2025. arXiv:2501.15498, doi:10.22323/1.474.0035.
- [70] A. Zhitnitsky, M. Maroudas, Mysterious anomalies in Earth’s atmosphere and strongly interacting Dark Matter, *Symmetry* 17 (2025) 79. arXiv:2405.04635, doi:10.3390/sym17010079.